European Journal of Medicinal Chemistry 218 (2021) 113341

Contents lists available at ScienceDirect

European Journal of Medicinal Chemistry

journal homepage: http://www.elsevier.com/locate/ejmech

# Discovery of thalidomide-based PROTAC small molecules as the highly efficient SHP2 degraders

Xiangbo Yang [a, d, 1], Zhijia Wang [b, c, 1], Yuan Pei [a, d], Ning Song [b, d, e], Lei Xu [b], Bo Feng [b, f], Hanlin Wang [b, g], Xiaomin Luo [b, h], Xiaobei Hu [b], Xiaohui Qiu [b], Huijin Feng [a], Yaxi Yang [a, d, i], Yubo Zhou [b, d, **], Jia Li [b, d, e, f, h, ***], Bing Zhou [a, d, i, *]

[a] Department of Medicinal Chemistry, State Key Laboratory of Drug Research, Shanghai Institute of Materia Medica, Chinese Academy of Sciences, Shanghai, 201203, China
[b] National Center for Drug Screening, State Key Laboratory of Drug Research, Shanghai Institute of Materia Medica, Chinese Academy of Sciences, Shanghai, 201203, China
[c] School of Pharmaceutical Science, Jiangnan University, Wuxi, 214122, China
[d] University of Chinese Academy of Sciences, 19 Yuquan Road, Beijing, 100049, China
[e] ShanghaiTech University, 393 Middle Huaxia Road, Shanghai, 201210, China
[f] School of Life Science and Biopharmaceutics, Shenyang Pharmaceutical University, No.103 Wenhua Road, Shenyang, Liaoning, China
[g] School of Pharmacy, Fudan University, Shanghai, 201203, China
[h] School of Chinese Materia Medica, Nanjing University of Chinese Medicine, Nanjing, 210046, China
[i] School of Pharmaceutical Science and Technology, Hangzhou Institute for Advanced Study, University of Chinese Academy of Sciences, Hangzhou, 310024, China

ARTICLE INFO

*Article history:*
Received 7 December 2020
Received in revised form
8 February 2021
Accepted 25 February 2021
Available online 11 March 2021

*Keywords:*
SHP2 degradation
Proteolysis targeting chimera (PROTAC)
Thalidomide-based heterobifunctional molecules
E3 ubiquitin ligase
CRBN

ABSTRACT

SHP2, a non-receptor tyrosine phosphatase, plays a pivotal role in numerous oncogenic cell-signaling cascades like RAS-ERK, PI3K-AKT and JAK-STAT. On the other hand, proteolysis targeting chimera (PROTAC) has emerged as a promising strategy for the degradation of disease-related protein of interest (POI). SHP2 degradation via the PROTAC strategy will provide an alternative startegy for SHP2-mediated cancer therapy. Herein we described the design, synthesis and evaluation of a series of thalidomide-based heterobifunctional molecules and identified **11**(**ZB-S-29**) as the highly efficient SHP2 degrader with a $DC_{50}$ of 6.02 nM. Further mechanism investigation illustrated that **11** came into function through targeted SHP2 protein degradation.



## 1. Introduction

Src homology 2 (SH2) domain-containing phosphotase2 (SHP2), a non-receptor tyrosine phosphatase encoded by PTPN11 participates in numerous oncogenic cell-signaling cascades, such as RAS-ERK, PI3K-AKT and JAK-STAT [1–4]. Hyperactivation of SHP2 caused by somatic or germline mutation in PTPN11 has been validated in several kinds of human diseases, including Noonan syndrome [5], hematological malignancies like juvenile myelomonocytic leukemia(JML), myelodysplastic syndromes(MDS), acute myeloid leukemia(AML) [6,7], and solid tumors [8]. Moreover, accumulating evidence has shown that SHP2 may play an important role in the immune evasion and in the T-cell programed cell death/checkpoint pathway (PD1/PD-L1) [9]. Given the promising importance of SHP2

* Corresponding author. Department of Medicinal Chemistry, State Key Laboratory of Drug Research, Shanghai Institute of Materia Medica, Chinese Academy of Sciences, Shanghai, 201203, China.
** Corresponding author. National Center for Drug Screening, State Key Laboratory of Drug Research, Shanghai Institute of Materia Medica, Chinese Academy of Sciences, Shanghai, 201203, China.
*** Corresponding author. National Center for Drug Screening, State Key Laboratory of Drug Research, Shanghai Institute of Materia Medica, Chinese Academy of Sciences, Shanghai, 201203, China.;
*E-mail addresses:* ybzhou@simm.ac.cn (Y. Zhou), jli@simm.ac.cn (J. Li), zhoubing@simm.ac.cn (B. Zhou).
[1] These authors contributed equally.

https://doi.org/10.1016/j.ejmech.2021.113341
0223-5234/

protein in clinical therapy, great efforts from both the academic and industrial communities have been devoted to the discovery of highly potent, selective and orally bioavailable SHP2 inhibitors [10]. Recently, the first SHP2 inhibitor with good selectivity and cellular activity was discovered by the scientists from Novartis, through targeting the tunnel-like allosteric binding pocket [11,12]. Subsequent optimization finally yielded another two structurally distinct candidates SHP394 [13] and SHP389 [14] as shown in Fig. 1. And by now, several SHP2 inhibitors, with TNO155 [15] and JAB-3068 (Fig. 1) as the representatives have entered into phase Ito IIclinical trials for the treatment of colorectal cancer, digestive/gastrointestinal cancer, head and neck cancer, etc.

About two decades ago, proteolysis targeting chimera (PROTAC) strategy was put forward by Crews and Deshaies etc to achieve targeted protein degradation [16]. A PROTAC molecule is composed of three fragments: two ligands each binding the protein of interest (POI) and E3 ligase complex respectively and one linker tethering the two ligands together. By hijacking the E3 ligase, the PROTAC molecules induce the ubiquitination of targeted proteins and lead to subsequent degradation. Over the past few years, PROTAC approach has been applied to the degradation of a range of disease-causing proteins like kinases [17–20], epigenetic readers or erasers [21–25], nuclear receptors [26–28], transcription fctors [29,30] and some others [31,32]. Of note, the PROTAC strategy has illustrated great advantages over the traditional occupy-driven target inhibition mechanism. Contrast to the occupy-based therapeutics which requires high in vivo concentrations to ensure sufficient target engagement, the event-driven PROTAC acts catalytically [33,34], thus potentially abolishing the potential off-target effects or toxicity and also being able to achieve greater cellular potencies in the inhibition of the target protein function than their corresponding inhibitors. In addition, PROTAC is of great promise to target the currently undruggable proteins including those lacking an active pocket for inhibitors to bind or others functioning as a scaffold, which is not addressable by inhibitors. Finally, PROTAC strategy can overcome drug resistance associated with traditional inhibitors.

Recently, the group of Ruess reported that knockout of the PTPN11 gene, encoding SHP2, in KRAS mutant human ductal adenocarcinoma cells leads to a reduction in cell proliferation [35]. Very Recently, the first SHP2 degrader SHP-D26 was reported, which induced rapid and efficient SHP2 degradation [36]. SHP2-D26 employed VHL-1 ligand for E3 ligase complex recruiting. Previous studies have demonstrated that the same protein could be degraded by utilizing different ubiquitin/proteasome systems(UPS) [21,37]. Moreover, the degradation efficiency has different dependence on CRBN and VHL ligases in different cells and thus the CRBN-based PROTAC degrader can be a good complement for VHL-based degrader. In this context, we wish to report the successful discovery of a series of novel SHP2 degraders with the thalidomide as the warhead to hijack the most widely expressed E3 ubiquitin ligase CRBN.

## 2. 2. results and discussion

PROTAC molecules design. Rational design of PROTAC molecules is mainly concerned about two elements, the ligands and the tethering site for linkers to anchor. Compound **7** (Fig. 2A), an analogue of TNO155, was a potent and selective SHP2 inhibitor ($IC_{50}$ = 17 nM), and therefore was employed as the suitable ligand for SHP2 protein recruiting. To expand the range of E3 ligase tool box for SHP2 degradation, we selected thalidomide as the binder for CRBN hijacking. Co-crystal structure of SHP2 complexed with TNO155 (PDB ID:7jvm) illustrated that the substituted pyridine moiety was solvent exposed (Figure 2B), which provided an opportunity for linker tethering. Accordingly, we designed the putative PROTAC molecules by connecting thalidomide part and the amino group of SHP2 binder **7** with a linker as shown in Fig. 2C.

Linker length exploration. As has been detailed previously, linker length plays a key role in degradation efficiency. To determine the acceptable or optimal linker length, we systematically varied the linker length in compounds **8**–**11** (Table 1). Preliminary evaluation of their ability to induce SHP2 protein degradation was carried out in MV4; 11 cell line by Western blotting (Fig. 3A), and the percentages of SHP2 protein degradation at two indicated concentrations were summarized (Table 1). Compound **8** with a five atoms long chain as the linker had extremely weak influence on SHP2 level at the concentration of 8 nM. But when at 200 nM, **8** successfully induced SHP2 protein degradation by more than 20%. Increasing the length by a $-(CH_2)_2O-$ moiety led to **9** which induced 25% and 37% decrease of SHP2 level at the concentration of 8 nM and 200 nM respectively. Further extension of the linker by two $-(CH_2)_2O-$ moieties yielded **10**. Despite almost no increase of degradation efficacy was obtained compared with **9** at 8 nM, **10** induced apparent SHP2 level reduction by 67% at the high concentration of 200 nM. Inspired by the phenomenon that longer linker performed better, we further increased the length of the linker by two methylenes relative to **10** and got **11**(**ZB-S-29**) which exhibited promising potency in inducing SHP2 degradation by 46% at the concentration of as low as 8 nM and by 85% at 200 nM.

Tethering site exploration. The structure of the DDB1-CRBN E3 ubiquitin ligase complexed with thalidomide has revealed that C5 position, as well as the C4 was exposed to the solvent region [38], which makes the C5 position another suitable site for linker tethering. To make an intuitive head-to-head comparison, linkers used in Table 1 were installed to the C5 position of thalidomide, yielding **12**–**15** respectively. The same procedures performed for the evaluation of these degraders were carried out (Fig. 3B) and data was summarized and displayed in Table 2. The discipline summarized from Table 2 was almost the same to that from Table 1. The

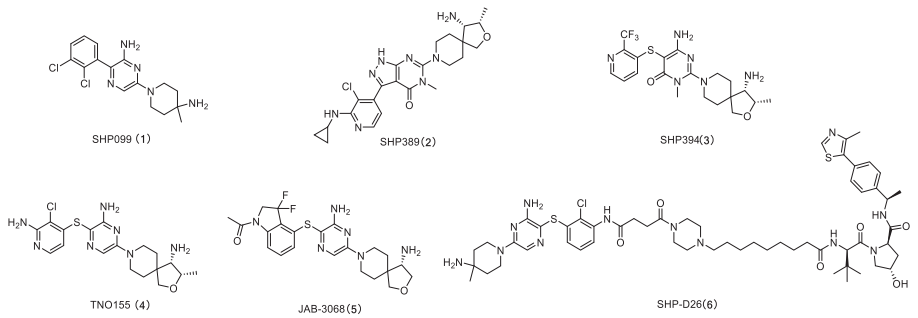


**Fig. 1.** Chemical structures of representative SHP2 allosteric inhibitors (**1**–**5**) and VHL-based SHP2 degrader (**6**, SHP2-D26).

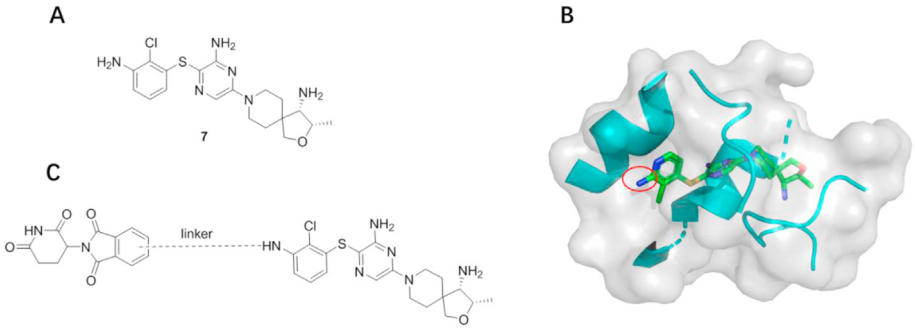


**Fig. 2.** Design of the PROTAC molecules. (A) Chemical structure of SHP2 binder **7**. (B) Co-crystal structure of SHP2 complexed with TNO155. The amino group was oriented toward the solvent and circled in red. (C) Putative PROTAC molecules.

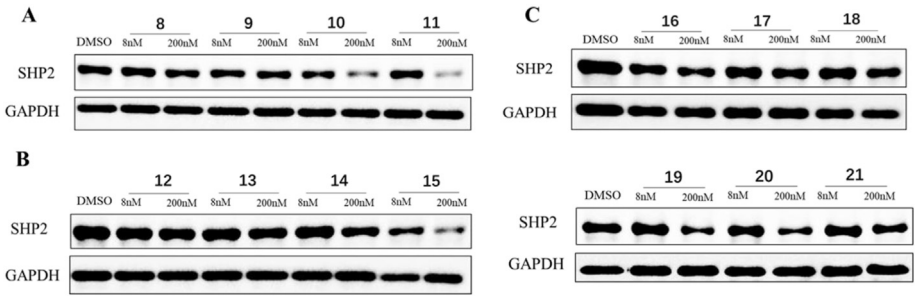


**Fig. 3.** Western blotting analysis of SHP2 protein in MV4; 11 cell lines treated with(A) **8**–**11,** (B) **12**–**15** and (C) **16**–**21** at indicated concentrations of 8 nM and 200 nM with a treatment period of 12 h. GAPDH was employed as the loading control. SHP2 protein levels at indicated concentrations were quantified and normalized over the corresponding GAPDH protein. Data were summarized in Tables 1–3 respectively.

degradation efficiency grew along with the increase of the linker length when these degraders were incubated with MV4; 11 cell line at the indicated concentration of 200 nM. Of note, all the four degraders in Table 2 were not as effective in inducing SHP2 protein reduction as their counterparts in Table 1. For example, both **13** and **14** induced less than 5% while their peers **9** and **10** successfully resulted in 25% and 28% of SHP2 degradation respectively at the low concentration of 8 nM. All of the above demonstrated that C5 position employed for linker tethering was tolerable for SHP2 degrader design but might not be the best choice as compared with C4 position.

Linker composition exploration. Large amounts of studies have demonstrated that chemical composition of a linker in one PROTAC molecule may greatly influence the degradative potency. Therefore, we replaced the polyethylene glycol linkers with full-carbon chains of 8−13 carbon atoms, giving another series of putative SHP2 protein degraders. As shown in Fig. 3C and Table 3, **19** with a linker of 11 carbon atoms long performed best among these six degraders with 73% of SHP2 protein degradation in MV4; 11 cell line at 200 nM but it was still less potent than **11** or **15**. Either extending or shortening the linker length resulted in the decrease of degradation efficiency. Compound **20**, with a linker one methylene longer appeared to be less potent than **19** while **18**, with a linker one methylene shorter than that of **19** failed to induced SHP2 degradation. Moreover, compound **21,** with the same linker length with **11** or **15,** was much less potent than **11**, indicating that linker composition also played an important role in degradation efficiency.

Does- and time-dependence study. Further examination of SHP2 protein degradation induced by **11** at a variety of concentrations was performed and western blotting results clearly illustrated that SHP2 protein levels were reduced in a dose-dependent manner (Fig. 4A), and qualification of the western blotting data gave the $DC_{50}$, the concentration required for 50% degradation of protein of interest, of 6.02 nM (Fig. 4B). In the following kinetic studies, MV4; 11 cell lines were incubated with 100 nM of **11**. Western blotting analysis at indicated time points demonstrated that SHP2 degradation induced by **11** proceeded in a time-dependent manner (Fig. 4C). 6 h's incubation led to >50% degradation, and much longer exposure for 24 h resulted in >90% SHP2 degradation.

Cell growth inhibition study. Next, we evaluated the activity of **11** on cell proliferation inhibition in MV4; 11 cell line (Fig. 5A). Interestingly, the excellent performance of **11** in SHP2 protein degradation didn't translate into impressive cell growth inhibition. Compared with the canonical inhibitor **SHP099**, compound 11 is only two times more potent in inhibiting cell growth. Cell cycle arrest and apoptosis studies revealed that **11** induced apparent G1 phase arrest or apoptosis in a dose-dependent manner(Fig. 5C and D). Moreover, cells treated with **11** suffered from more severe G1 phase arrest or apoptosis compared with those treated with **SHP099** at the same concentration of 200 nM, which was consistent with the fact that **11** was more potent in regard to cell growth inhibition than **SHP099**.

Mechanism of action study. To make the mechanism of action of **11** in SHP2 protein degradation clear, we treated MV4; 11 cell line with **11** alone or combined with the CRBN ligand pomalidomide or the SHP2 binder **7** (Fig. 6A). Western blotting analysis demonstrated that either pomalidomide or **7** prevented SHP2 degradation, indicating that simultaneous binding of the two ligands to their receptors respectively was required for the efficient SHP2 protein degradation. Moreover, engineered CRBN deficient MV4; $11^{CRBN/KO}$ cell line was constructed (Fig. 6B) and then employed to further clarify that SHP2 degradation induced by **11** was CRBN dependent. As expected, SHP2 protein depletion in MV4; $11^{CRBN/KO}$ was totally abolished (Fig. 6C). We also determined the $IC_{50}$ values of both the **11** and the positive control SHP099 for inhibiting the growth of

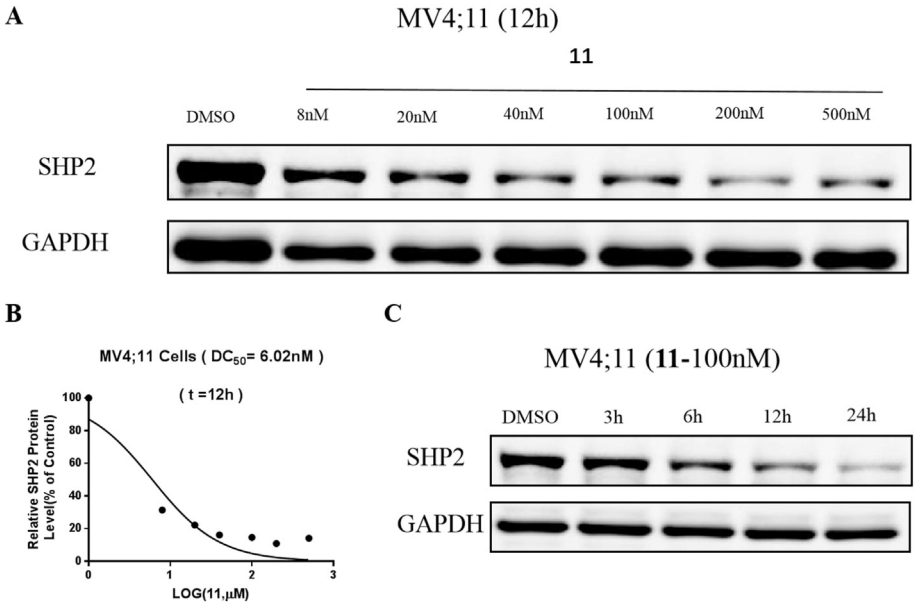


**Fig. 4.** Further examination of **11**. (A)Western blotting analysis of SHP2 protein in MV4; 11 cell line treated with **11** at indicated concentrations with a treatment period of 12 h. GAPDH was employed as the loading control. (B)Determination of $DC_{50}$ value of **11** in MV4; 11 cell line. SHP2 protein levels at indicated concentrations were quantified and normalized over the corresponding GAPDH protein. (C)Western blotting analysis of SHP2 protein in MV4; 11 cell line pretreated with 100 nM of **11** and harvested at indicated time points. GAPDH was employed as the loading control.

MV4; $11^{CRBN/KO}$ and MV4; $11^{WT}$ cell lines (Fig. 6D and E). Contrast to the observation that SHP099 behaved a little more potent in MV4; $11^{CRBN/KO}$ than in MV4; $11^{WT}$, **11** showed a ten times less potent in the growth inhibition of CRBN-knocked off MV4; 11 cell line than that of the wide type MV4; 11 cell line, which might be attributed to the CRBN deficiency and SHP2 delegation abolishment. **PS-341**, one unique and specific proteasome inhibitor [39], recovered SHP2 protein level as well (Fig. 6A). In summary, **11** was a bona fide PROTAC molecule and came into function by inducing SHP2 degradation.

## 3. Chemistry

The synthesis of the key intermediates or fragments and the final PROTAC molecules is briefly described as follows.

### 3.1. Synthesis of fragment *30*

The synthesis of fragment **30** as shown in Scheme 1 has already been described in related patents(WO 2016203406) and alternative approaches(WO 2020065452, WO 2020065453) are also available now.

Reagents and conditions: (a)TBSCl, imidazole, DCM, r.t., 12 h; (b) DIBAL-H, ether, −78 °C, 2 h; (c)n-BuLi, diethylamine, THF, −78 °C, 2 h; (d)$LiBH_4$, THF, r.t., 24 h; (e)1 M TBAF in THF, THF, r.t., 5 h; (f)NaH, Tosyl chloride, THF, 0 °C, 3 h; (g)Dess-Martin periodinane, DCM, r.t., 5 h; (h)Titanium ethoxide, (R)-(+)-2-methyl-propanesulfinamide, THF, reflux, 24 h; (i)$LiBH_4$, THF, 0 °C to r.t.; (j)4 M HCl in dioxane, 50 °C, 12 h.

### 3.2. Synthesis of the key intermediate *35*

The synthetic route to the key intermediate **35** is described as follows(Scheme 2). The 3-amino-2-chlorobenzenethiol precursor **31** was synthesized via a $S_NAr$ reaction between the 2-chloro-3-fluoroaniline and 2-methylpropane-2-thiol. Removal of the tertiary butyl in concentrated hydrochloric acid afforded the 3-amino-2-chlorobenzenethiol hydrochloride **32**, which was employed as the reagent to construct the intermediate **33** via PdCu-catalyzed cross coupling reaction. Subsequent nucleophilic substitution between **33** and the amine fragment **30** gave **7**(that is the SHP2 binder employed here for PROTAC molecules design). After the aliphatic amine was selectively protected with a Boc moiety, succinic acid was then installed to the aromatic amine, finally yielding the key intermediate **35**.

Reagents and conditions: (a)$CsCO_3$, DMF, 120 °C, 24 h; (b)Conc. HCl, 50 °C, 24 h; (c)CuI, O-Phenanthroline, $K_3PO_4$, dioxane, 85 °C, 5 h; (d)DIPEA, DMSO, 120 °C, 12 h; (e)tert-butyldicarbonate, DIPEA, DCM/DMF; (f)Succinic anhydride, toluene, 110 °C, 5 h.

### 3.3. Synthesis of the key intermediates *37*–*50*

Other key intermediates **37**–**50** were prepared amid a general synthetic route of two steps as shown in Scheme 3 and Scheme 4. The fluorine-substituted thalidomide analogue **36a/b** was synthesized from commercially available 3- or 5-fluorophthalic anhydride and 2,6-dioxopiperidine-3-ammonium chloride almost quantitatively. Linkers of different length and composition were then installed to the phenyl ring in placement of the fluorine via aromatic nucleophilic substitution to provide these intermediates **37**–**50**.

### 3.4. Synthesis of the SHP2 degraders *8*–*21*

The target PROTAC molecules were prepared through the synthetic route outlined in Scheme 5. The protecting Boc groups of intermediates **37**–**50** were removed with TFA first and subsequent amide condensation between the individual TFA salt and another key intermediate **35** gave the PROTAC molecule precursors **51**–**64** respectively. De-protection of these precursors with TFA finally afforded the fourteen degraders **8**–**21**.

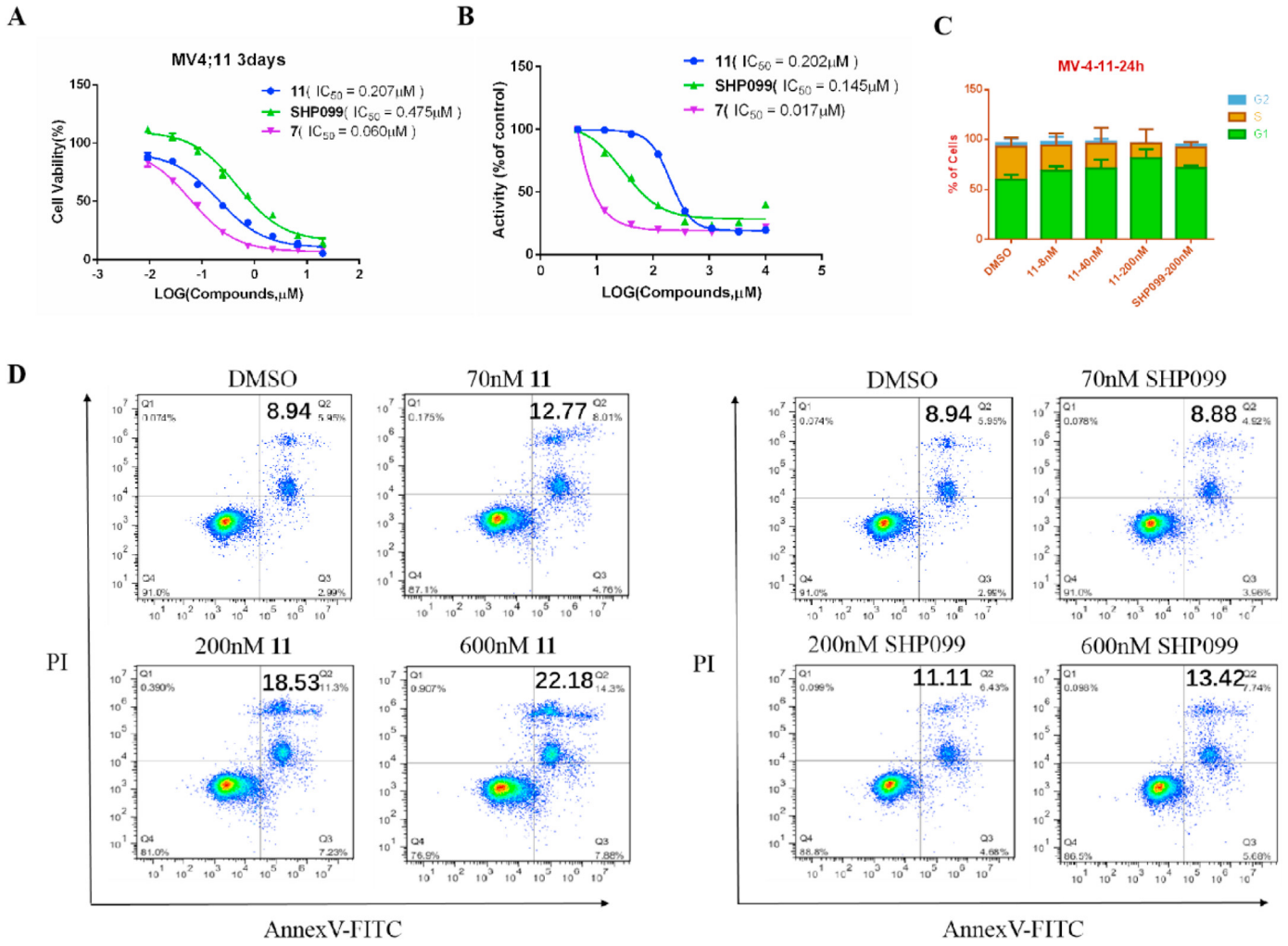


**Fig. 5.** Evaluation of **11** in cell growth inhibition. (A)MV4; 11 cell growth inhibition by the treatment of **11**, SHP099 and **7**. MV4; 11 cells were treated with individual compound at indicated doses for 3d and cell viability was determined by MTS. (B)SHP2 catalytic activity inhibition by the treatment of **11**, SHP099, and **7**. (C)Cell cycle arrest induced by **11** or SHP099. MV4; 11 cells were treated with **11** or SHP099 at indicated doses for 24 h before analysis. (D)Cell apoptosis induced by **11** or SHP099. MV4; 11 cells were treated with **11** or SHP099 at indicated doses for 48 h. Cell cycle and cell apoptosis analysis were performed by FlowJo software (Tree Star, Inc.).

## 4. Conclusion and outlook

In summary, we designed a series of thalidomide-based SHP2 degraders by employing CRBN ligand for E3 ligase complex recruiting. Key elements namely linker length, linker tethering site and linker compositions were explored and finally compound **11**(**ZB-S-29**) was identified as the most potent SHP2 degrader. Western blotting analysis indicated that (1)SHP2 protein could be degraded by hijacking CRBN, (2)the C4 position of thalidomide was the better choice for linker tethering as compared with C5 and (3) full-carbon chains didn't benefit SHP2 degradation relative to the polyethylene glycol (PEG) linkers. Further exploration showed that **11** effectively induced SHP2 protein degradation in a time- and dose-dependent manner and achieved a $DC_{50}$ of 6.02 nM. Further mechanism investigation illustrated that **11** came into function through targeted SHP2 protein degradation. We believe that **11** may have futher potential application as a probe for the exploration of physiological functions of SHP2, which is complementary to other techniques like gene editing or RNAi.

## 5. Materials and methods

### 5.1. Synthesis

**3-(tert-butylthio)-2-chloroaniline(31)** To a solution of 2-chloro-3-fluorobenzenamin (5 g, 34.35 mmol) and 2-Methyl-2-propanethiol (9.29 g, 103 mmol) in DMF (80 mL) was added $Cs_2CO_3$(16.79 g, 51.53 mmol) and the mixture was heated at 120 °C for 24 h. After cooling to room temperature, the reaction was poured into a separating funnel containing sat. aq. $NH_4Cl$ (150 mL) and extracted with EtOAc (100 mL*3). The combined organics were washed with brine and dried over $Na_2SO_4$. Then the volatiles were removed under reduced pressure and the resulting residue was purified by flash chromatography to give **31** in 83% yield. UPLC-MS:$[M+H]^+$ = 215.86/217.65 found. $^1$H NMR (400 MHz, Chloroform-*d*) δ 7.04 (dd, *J* = 7.6, 2.0 Hz, 1H), 7.01 (t, *J* = 7.6 Hz, 1H), 6.77 (dd, *J* = 7.5, 2.0 Hz, 1H), 4.16 (s, 2H), 1.33 (s, 9H).

**3-amino-2-chlorobenzenethiol hydrochloride(32)** 3-(tert-butylthio)-2-chloroaniline(**31**) (5 g, 23 mmol) was suspended in

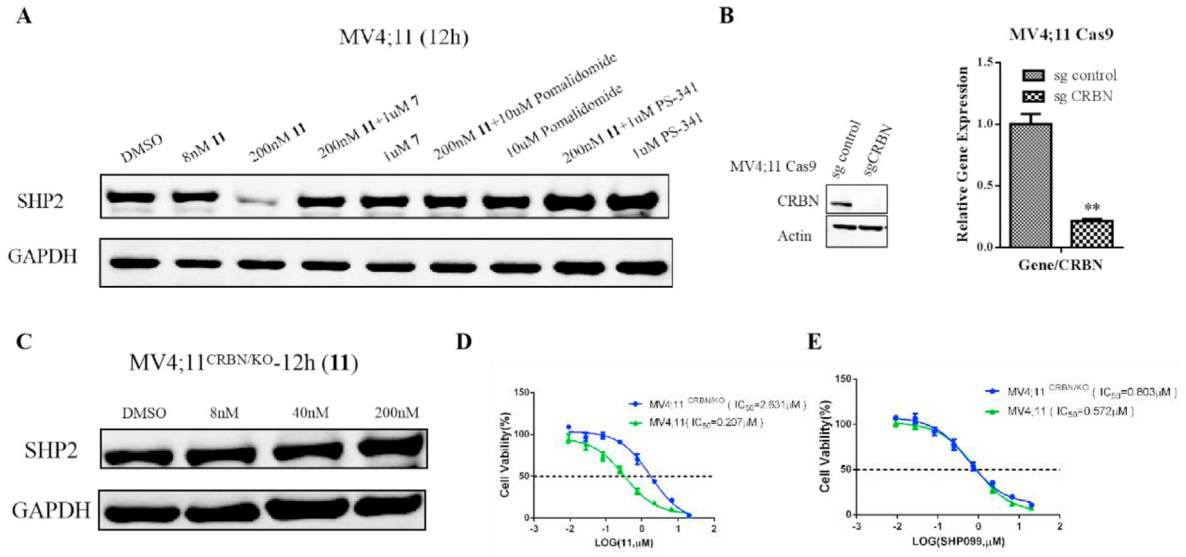


**Fig. 6.** Mechanism of action study of **11**. (A)Western blotting analysis of SHP2 protein in MV4; 11 cell line. Cells were treated with CRBN ligand pomalidomide, SHP2 inhibitor **7**, or proteasome inhibitor **PS-341** 2 h before the treatment with **11** for another 12 h. (B)Verification of the construction of CRBN-deficient MV4; 11 cell line. (C)Western blotting analysis of SHP2 protein in MV4; $11^{CRBN/KO}$ cell line treated with **11** at indicated concentrations with a treatment period of 12 h. GAPDH was employed as the loading control. (D, E)MV4; 11 or MV4; $11^{CRBN/KO}$ cell growth inhibition by the treatment of **11**(D) and SHP099(E). Cells were treated with individual compound at indicated doses for 3d and cell viability was determined by MTS.

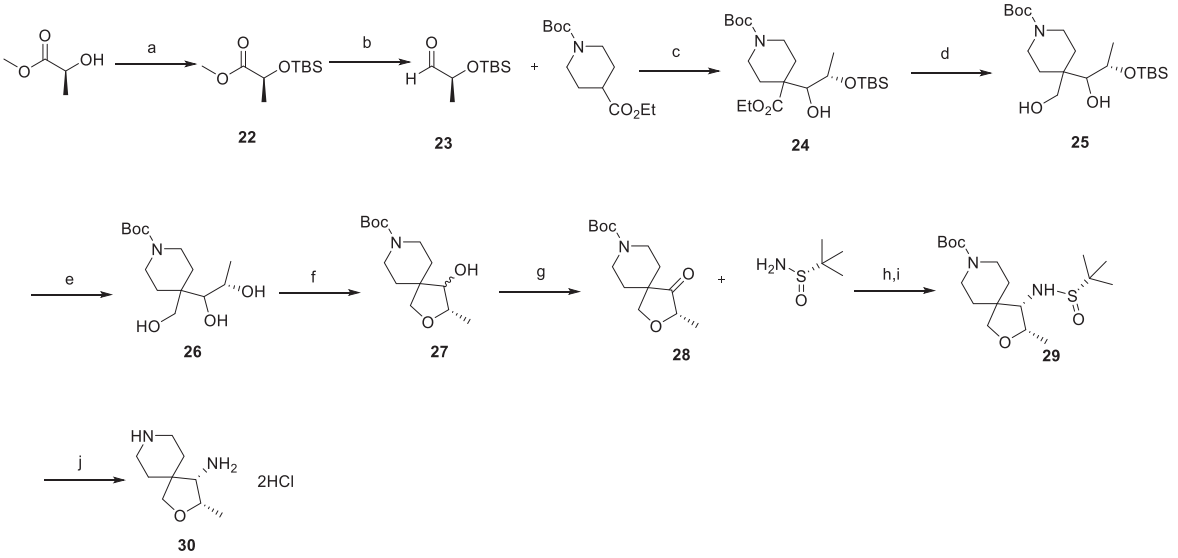


**Scheme 1.** Synthetic route to intermediate 30.

concentrated hydrochloric acid(30 mL) and the slurry was heated at 50 °C for 24 h. After that, volatiles were removed under reduced pressure and the 3-amino-2-chlorobenzenethiol hydrochloride was obtained as white powers which was used directly in the next step without further purification. UPLC-MS:$[M+H]^+$ = 159.56/161.48 found.

**3-((3-amino-2-chlorophenyl)thio)-6-chloropyrazin-2-amine(33)** To a solution of 3-bromo-6-chloropyrazin-2-amine (1.00 g, 4.80 mmol) and 3-amino-2-chlorobenzenethiol hydrochloride(**32**) (1.04 g, 5.28 mmol) in dioxane (25 mL) was added $K_3PO_4$ (2.03 g, 9.60 mmol), CuI (182 mg, 0.96 mmol) and o-Phenanthroline (346 mg, 1.92 mmol). The mixture was degassed and refilled with nitrogen three times and was then heated at 85 °C for 3 h. After that the solvents were removed under reduced pressure and the resulting residue was purified by flash chromatography to give **33** as light yellow solids in 70% yield. UPLC-MS:$[M+H]^+$ = 286.71/288.63/290.59 found. $^1$H NMR (400 MHz, DMSO-$d_6$) δ 7.69 (s, 1H), 7.02–6.95 (m, 3H), 6.78 (dd, $J$ = 8.1, 1.5 Hz, 1H), 6.49 (dd, $J$ = 7.6, 1.4 Hz, 1H), 5.53 (s, 2H).

**(3S,4S)-8-(6-amino-5-((3-amino-2-chlorophenyl)thio)pyrazin-2-yl)-3-methyl-2-oxa-8-azaspiro[4.5]decan-4-amine(7)** To a solution of **33** (500 mg, 1.74 mmol) and **30** (550 mg, 2.26 mmol) in DMSO (15 mL) was added DIPEA (2.88 mL, 17.41 mmol) and the mixture was heated at 120 °C for 12 h. After cooling to room temperature, the mixture was poured into a separating funnel containing sat. aq. $NH_4Cl$ (30 mL) and extracted with EtOAc (20 mL*3). The combined organics were washed with brine and dried over $Na_2SO_4$. Then the volatiles were removed under reduced

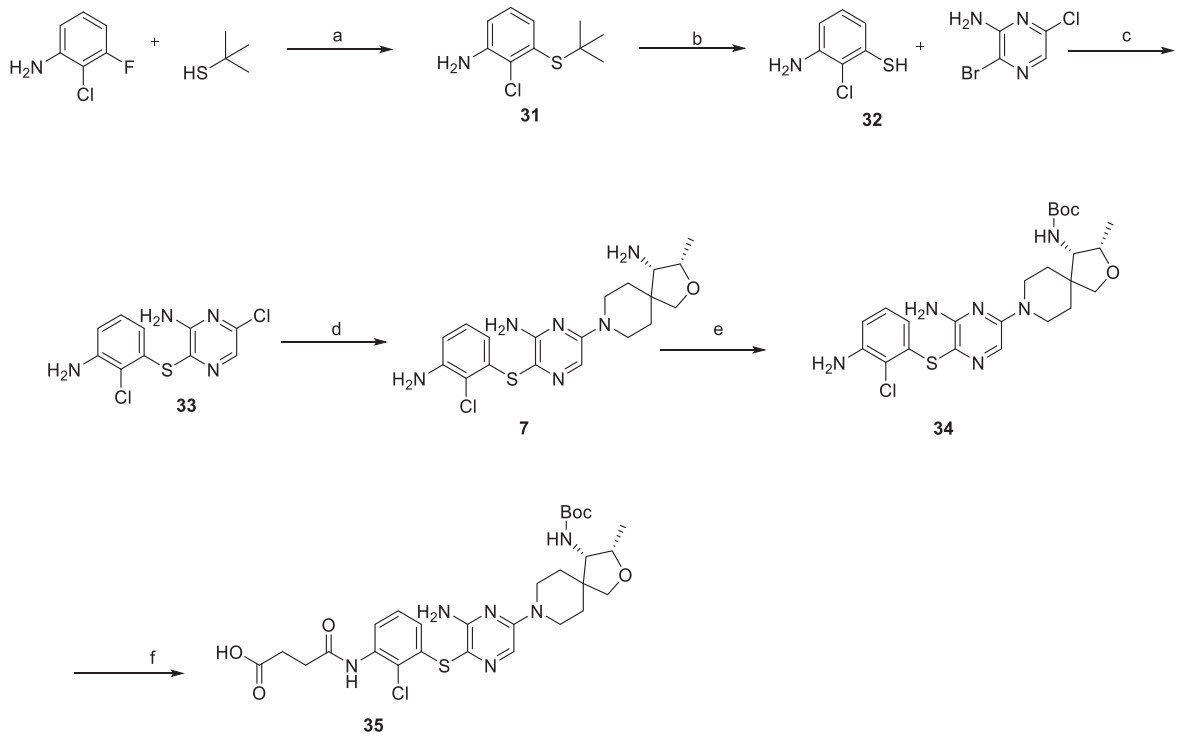

**Scheme 2.** Synthetic route to the key intermediate **35**.

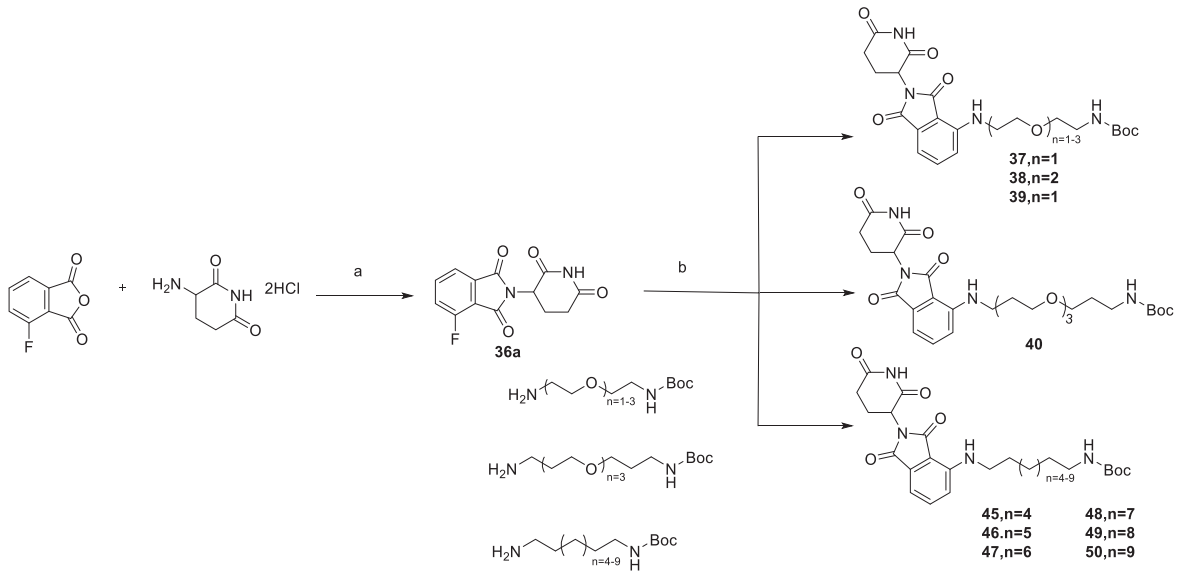

**Scheme 3.** Synthetic route to the key intermediates **37**–**40** and **45**–**50**. Reagents and conditions: (a)KOAc, AcOH, 120 °C, 12 h; (b)DIPEA, DMAc, 90 °C, 2 h.

pressure and the resulting residue was purified by flash chromatography to give **7** as white solids in 67% yields. UPLC-MS:$[M+H]^+$ = 421.20/422.91 found. $^1$H NMR (400 MHz, Chloroform-*d*) δ 7.61 (s, 1H), 6.86 (t, *J* = 7.9 Hz, 1H), 6.54 (dd, *J* = 7.9, 1.4 Hz, 1H), 6.19 (dd, *J* = 7.9, 1.4 Hz, 1H), 4.86 (s, 2H), 4.18 (qd, *J* = 6.4, 4.4 Hz, 1H), 4.10 (s, 2H), 3.93–3.81 (m, 2H), 3.79 (d, *J* = 8.7 Hz, 1H), 3.68 (d, *J* = 8.7 Hz, 1H), 3.38 (ddd, *J* = 13.3, 8.6, 4.3 Hz, 1H), 3.28 (ddd, *J* = 13.2, 9.5, 3.4 Hz, 1H), 2.98 (d, *J* = 4.5 Hz, 1H), 1.83 (ddd, *J* = 13.4, 9.5, 3.9 Hz, 1H), 1.77–1.59 (m, 2H), 1.57–1.51 (m, 1H), 1.23 (d, *J* = 6.4 Hz, 3H).

**tert-butyl ((3S,4S)-8-(6-amino-5-((3-amino-2-chlorophenyl) thio)pyrazin-2-yl)-3-methyl-2-oxa-8-azaspiro[4.5]decan-4-yl) carbamate(34)** To a solution of **7** in the mixture of DCM (10 mL) and DMF (0.5 mL) was added $Boc_2O$, and the reaction was stirred at room temperature for 36 h. After that, the volatiles were removed under reduced pressure and the residues were purified by flash chromatography to provide **34** as white solids in 73% yield. UPLC-MS:$[M+H]^+$ = 521.23/523.11 found. $^1$H NMR (400 MHz, Chloroform-*d*) δ 7.58 (s, 1H), 6.87 (t, *J* = 7.9 Hz, 1H), 6.54 (dd, *J* = 8.0, 1.4 Hz, 1H), 6.18 (dd, *J* = 7.9, 1.4 Hz, 1H), 4.84 (s, 2H), 4.66 (d, *J* = 10.7 Hz,

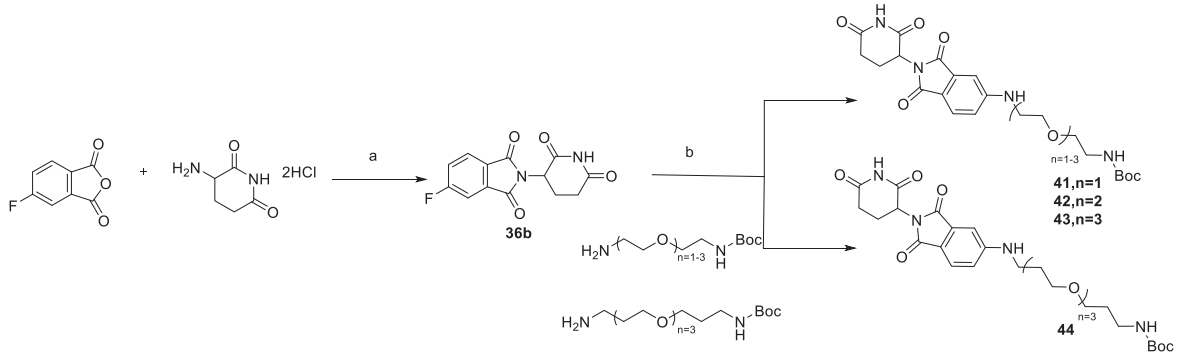


**Scheme 4.** Synthetic route to the key intermediates **41**–**44**. Reagents and conditions: (a)KOAc, AcOH, 120 °C, 12 h; (b)DIPEA, DMAc, 90 °C, 2 h.

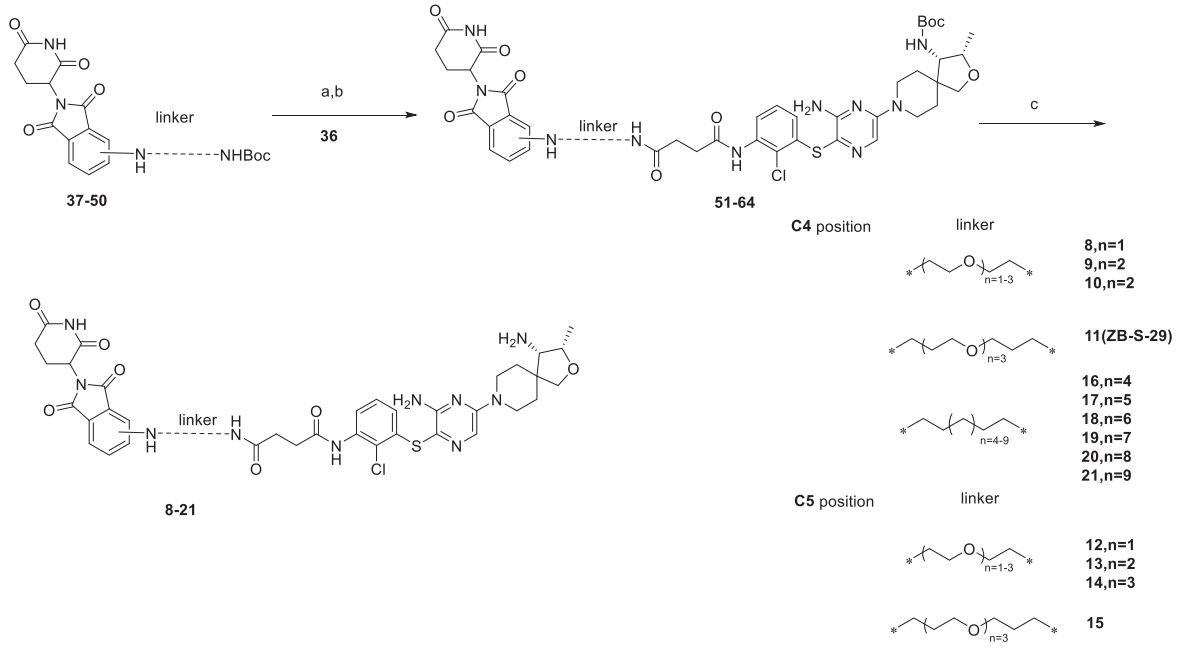


**Scheme 5.** Synthetic route to SHP2 degraders 8 to 21. Reagents and conditions: (a)TFA/DCM, r.t., 1 h; (b)HATU, DIPEA, DMF, r.t., 3 h; (c)TFA/DCM, r.t., 1 h.

1H), 4.20–4.13 (m, 1H), 4.10 (s, 2H), 3.98 (dd, $J$ = 10.8, 4.3 Hz, 1H), 3.85–3.60 (m, 4H), 3.51 (ddd, $J$ = 13.0, 8.0, 3.6 Hz, 1H), 3.38 (ddd, $J$ = 12.8, 8.3, 3.5 Hz, 1H), 1.91–1.65 (m, 3H), 1.66–1.51 (m, 1H), 1.44 (s, 9H), 1.19 (d, $J$ = 6.3 Hz, 3H).

**4-((3-((3-amino-5-((3S,4S)-4-((tert-butoxycarbonyl)amino)-3-methyl-2-oxa-8-azaspiro[4.5]decan-8-yl)pyrazin-2-yl)thio)-2-chlorophenyl)amino)-4-oxobutanoic acid(35)** To a suspension of **34** (300 mg, 0.58 mmol) in toluene (10 mL) was added succinic anhydride (69 mg, 0.69 mmol) and the mixture was refluxed for 6 h. Then the volatiles were removed under reduced pressure and the resulting residue was purified by Prep HPLC with MeCN/$H_2O$ as the eluent and 1% of ammonia liquor as modifier to give **35** as white solids in 83% yield. UPLC-MS:$[M+H]^+$ = 621.48/623.19 found. $^1$H NMR (400 MHz, Methanol-$d_4$) δ 7.55 (s, 1H), 7.11 (t, $J$ = 8.0 Hz, 1H), 7.01 (d, $J$ = 10.5 Hz, 1H), 6.53 (dd, $J$ = 8.0, 1.4 Hz, 1H), 4.31–4.21 (m, 1H), 3.98 (dd, $J$ = 10.7, 4.7 Hz, 1H), 3.83–3.52 (m, 6H), 2.78–2.71 (m, 2H), 2.67 (t, $J$ = 6.5 Hz, 2H), 1.88–1.68 (m, 3H), 1.67–1.52 (m, 1H), 1.46 (s, 9H), 1.15 (d, $J$ = 6.3 Hz, 3H).

**2-(2,6-dioxopiperidin-3-yl)-4-fluoroisoindoline-1,3-dione (36a)** To a solution of 3-Fluorophthalic anhydride (3 g, 18.06 mmol) and 2,6-Dioxopiperidine-3-ammonium chloride(3.27 g, 19.87 mmol) in acetic acid (30 mL) was added KAc (5.32 g, 54.2 mmol) and the mixture was heated at 120 °C for 12 h. After cooling to room temperature, the solution was poured into 200 mL of ice water. The participants were filtered and washed with cold water to provide **36a** as gray solids in 95% yield. UPLC-MS:$[M+H]^+$ = 317.07 found. $^1$H NMR (400 MHz, DMSO-$d_6$) δ 11.17 (s, 1H), 8.00–7.88 (m, 1H), 7.82–7.67 (m, 2H), 5.17 (dd, $J$ = 12.9, 5.3 Hz, 1H), 3.00–2.81 (m, 1H), 2.71–2.43 (m, 2H), 2.15–1.98 (m, 1H).

**2-(2,6-dioxopiperidin-3-yl)-5-fluoroisoindoline-1,3-dione(36b) 36b** was obtained according to the procedures described for **36a**. As gray solids in 92% yield. UPLC-MS:$[M+H]^+$ = 316.94 found. $^1$H NMR (400 MHz, DMSO-$d_6$) δ 11.16 (s, 1H), 8.01 (dd, $J$ = 8.3, 4.5 Hz, 1H), 7.85 (dd, $J$ = 7.4, 2.3 Hz, 1H), 7.75–7.69 (m, 1H), 5.17 (dd, $J$ = 12.8, 5.4 Hz, 1H), 2.90 (ddd, $J$ = 16.8, 13.7, 5.4 Hz, 1H), 2.69–2.43 (m, 2H), 2.15–1.99 (m, 1H).

**tert-butyl (2-(2-((2-(2,6-dioxopiperidin-3-yl)-1,3-dioxoisoindolin-4-yl)amino)ethoxy)ethyl)carbamat(37)** To a solution of **36a** (100 mg, 0.36 mmol) and tert-butyl (2-(2-aminoethoxy)ethyl)carbamate (78 mg, 0.38 mmol) in NMP (3 mL) was added DIPEA(180 μL, 1.09 mmol) and the mixture was heated at

**Table 1**
Exploration of the effect of linker length on degradation efficiency.

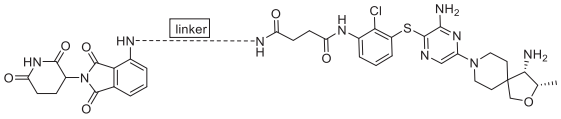


| Compound | Linker | % of SHP2 degradation in MV4; 11 cell line[a] | |
|---|---|---|---|
| | | 8 nM | 200 nM |
| **8** | 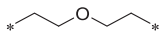 | 6 | 23 |
| **9** | 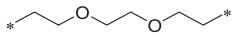 | 25 | 37 |
| **10** | 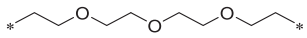 | 28 | 62 |
| **11** (**ZB-S-29**) | 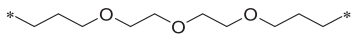 | 46 | 80 |

[a] % of SHP2 degradation at two indicated concentrations were expressed as the average of two independent measurements with a treatment period of 12 h in MV4; 11 cell line.

**Table 2**
Exploration of the effect of tethering site on degradation efficiency.

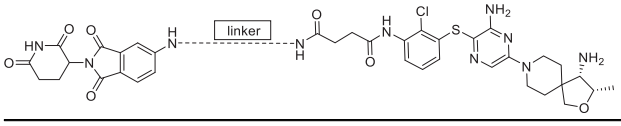


| Compound | Linker | % of SHP2 degradation in MV4; 11 cell line[a] | |
|---|---|---|---|
| | | 8 nM | 200 nM |
| **12** | 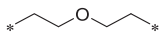 | 5< | 12 |
| **13** | 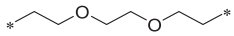 | 5< | 28 |
| **14** | 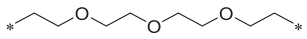 | 5< | 48 |
| **15** | 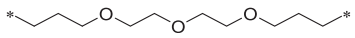 | 42 | 78 |

[a] % of SHP2 degradation at two indicated concentrations were expressed as the average of two independent measurements with a treatment period of 12 h in MV4; 11 cell line.

90 °C for 2 h. After cooling to room temperature, the mixture was poured into a separating funnel containing sat. aq. $NH_4Cl$ (15 mL) and extracted with EtOAc (30 mL). The combined organics were washed with brine and dried over $Na_2SO_4$. Then the volatiles were removed under reduced pressure and the resulting residue was purified by flash chromatography to give **37** as yellow solids in 67% yield. UPLC-MS:$[M+H]^+$ = 461.10 found. $^1$H NMR (400 MHz, Methanol-$d_4$) δ 7.53 (dd, $J$ = 8.6, 7.1 Hz, 1H), 7.07 (d, $J$ = 8.6 Hz, 1H), 7.04 (d, $J$ = 7.1 Hz, 1H), 5.05 (dd, $J$ = 12.6, 5.4 Hz, 1H), 3.68 (t, $J$ = 5.3 Hz, 2H), 3.53 (t, $J$ = 5.7 Hz, 2H), 3.48 (t, $J$ = 5.3 Hz, 2H), 3.23 (t, $J$ = 5.6 Hz, 2H), 2.92−2.65 (m, 3H), 2.15−2.06 (m, 1H), 1.41 (s, 9H).

Intermediates **38**−**50** were prepared following the same procedures described for the synthesis of **37** in 50%−71% yield.

**tert-butyl (2-(2-(2-((2-(2,6-dioxopiperidin-3-yl)-1,3-dioxoisoindolin-4-yl)amino)ethoxy)ethoxy)ethyl)carbamate(38)** As yellow solids. UPLC-MS:$[M+H]^+$ = 505.06 found. $^1$H NMR (400 MHz, Methanol-$d_4$) δ 7.54 (dd, $J$ = 8.5, 7.1 Hz, 1H), 7.07 (d, $J$ = 8.6 Hz, 1H), 7.04 (d, $J$ = 7.1 Hz, 1H), 5.06 (dd, $J$ = 12.5, 5.4 Hz, 1H), 3.72 (t, $J$ = 5.3 Hz, 2H), 3.68−3.58 (m, 4H), 3.55−3.44 (m, 4H), 3.21 (t, $J$ = 5.6 Hz, 2H), 2.94−2.64 (m, 3H), 2.22−2.05 (m, 1H), 1.40 (s, 9H).

**tert-butyl (2-(2-(2-(2-((2-(2,6-dioxopiperidin-3-yl)-1,3-dioxoisoindolin-4-yl)amino)ethoxy)ethoxy)ethoxy)ethyl)carbamate(39)** As yellow solids. UPLC-MS:$[M+H]^+$ = 549.13 found. $^1$H NMR (400 MHz, Methanol-$d_4$) δ 7.53 (dd, $J$ = 8.5, 7.2 Hz, 1H), 7.06 (d, $J$ = 8.6 Hz, 1H), 7.03 (d, $J$ = 7.1 Hz, 1H), 5.05 (dd, $J$ = 12.5, 5.4 Hz, 1H), 3.72 (t, $J$ = 5.3 Hz, 2H), 3.68−3.54 (m, 8H), 3.49 (q, $J$ = 5.3 Hz, 4H), 3.19 (t, $J$ = 5.6 Hz, 2H), 2.95−2.63 (m, 3H), 2.27−1.99 (m, 1H), 1.42 (s, 9H).

**tert-butyl (3-(2-(2-(3-((2-(2,6-dioxopiperidin-3-yl)-1,3-dioxoisoindolin-4-yl)amino)propoxy)ethoxy)ethoxy)propyl) carbamate(40)** As yellow solids. UPLC-MS:$[M+H]^+$ = 577.46 found. $^1$H NMR (400 MHz, Methanol-$d_4$) δ 7.52 (dd, $J$ = 8.6, 7.1 Hz, 1H), 7.04 (d, $J$ = 8.6 Hz, 1H), 7.01 (d, $J$ = 7.1 Hz, 1H), 5.04 (dd, $J$ = 12.6, 5.4 Hz, 1H), 3.70−3.52 (m, 10H), 3.48 (t, $J$ = 6.2 Hz, 2H), 3.42 (t, $J$ = 6.5 Hz, 2H), 3.10 (t, $J$ = 6.8 Hz, 2H), 2.94−2.62 (m, 3H), 2.11 (m, 1H), 1.90 (p, $J$ = 6.2 Hz, 2H), 1.70 (p, $J$ = 6.5 Hz, 2H), 1.42 (s, 9H).

**tert-butyl (2-(2-((2-(2,6-dioxopiperidin-3-yl)-1,3-dioxoisoindolin-5-yl)amino)ethoxy)ethyl)carbamate(41)** As yellow solids. UPLC-MS:$[M+H]^+$ = 461.08 found. $^1$H NMR (400 MHz, Methanol-$d_4$) δ 7.58 (d, $J$ = 8.4 Hz, 1H), 7.05 (d, $J$ = 2.2 Hz, 1H), 6.90 (dd, $J$ = 8.4, 2.2 Hz, 1H), 5.04 (dd, $J$ = 12.4, 5.4 Hz, 1H), 3.68 (t, $J$ = 5.3 Hz, 2H), 3.52 (t, $J$ = 5.5 Hz, 2H), 3.41 (t, $J$ = 5.3 Hz, 2H), 3.23 (t, $J$ = 5.3 Hz, 2H), 2.92−2.63 (m, 3H), 2.29−2.04 (m, 1H), 1.42 (s, 9H).

**tert-butyl (2-(2-(2-((2-(2,6-dioxopiperidin-3-yl)-1,3-dioxoisoindolin-5-yl)amino)ethoxy)ethoxy)ethyl)carbamate(42)** As yellow solids. UPLC-MS:$[M+H]^+$ = 505.14 found. $^1$H NMR (400 MHz, Methanol-$d_4$) δ 7.57 (d, $J$ = 8.4 Hz, 1H), 7.05 (d, $J$ = 2.2 Hz, 1H), 6.89 (dd, $J$ = 8.3, 2.2 Hz, 1H), 5.04 (dd, $J$ = 12.5, 5.5 Hz, 1H), 3.71 (t, $J$ = 5.4 Hz, 2H), 3.68−3.60 (m, 4H), 3.51 (t, $J$ = 5.6 Hz, 2H), 3.43 (t, $J$ = 5.4 Hz, 2H), 3.22 (t, $J$ = 5.6 Hz, 2H), 2.93−2.64 (m, 3H), 2.31−2.04 (m, 1H), 1.42 (s, 9H).

**Table 3**
Exploration of the effect of the full-carbon linker on degradation efficiency.

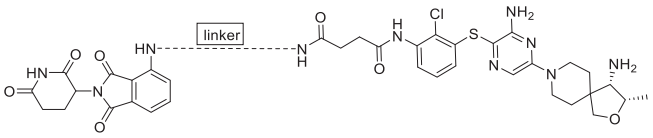


| Compound | Linker | % of SHP2 degradation in MV4; 11 cell line[a] | |
|---|---|---|---|
| | | 8 nM | 200 nM |
| **16** | 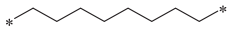 | 22 | 43 |
| **17** | 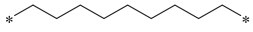 | 23 | 37 |
| **18** | 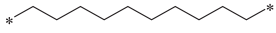 | 0 | 10 |
| **19** |  | 26 | 73 |
| **20** | 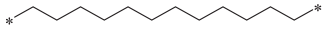 | 18 | 62 |
| **21** | 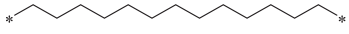 | 8 | 38 |

[a] % of SHP2 degradation at two indicated concentrations were expressed as the average of two independent measurements with a treatment period of 12 h in MV4; 11 cell line.

**tert-butyl (2-(2-(2-(2-((2-(2,6-dioxopiperidin-3-yl)-1,3-dioxoisoindolin-5-yl)amino)ethoxy)ethoxy)ethoxy)ethyl)carbamate(43)** As yellow solids. UPLC-MS:$[M+H]^+$ = 549.22 found. $^1$H NMR (400 MHz, Methanol-$d_4$) δ 7.57 (d, $J$ = 8.4 Hz, 1H), 7.05 (d, $J$ = 2.2 Hz, 1H), 6.90 (dd, $J$ = 8.4, 2.2 Hz, 1H), 5.04 (dd, $J$ = 12.5, 5.4 Hz, 1H), 3.71 (t, $J$ = 5.3 Hz, 2H), 3.68–3.57 (m, 8H), 3.50 (t, $J$ = 5.6 Hz, 2H), 3.42 (t, $J$ = 5.3 Hz, 2H), 3.21 (t, $J$ = 5.3 Hz, 2H), 2.94–2.63 (m, 3H), 2.30–2.04 (m, 1H), 1.42 (s, 9H).

**tert-butyl (3-(2-(2-(3-((2-(2,6-dioxopiperidin-3-yl)-1,3-dioxoisoindolin-5-yl)amino)propoxy)ethoxy)ethoxy)propyl) carbamate(44)** As yellow solids. UPLC-MS:$[M+H]^+$ = 577.48 found. $^1$H NMR (400 MHz, Methanol-$d_4$) δ 7.55 (d, $J$ = 8.3 Hz, 1H), 6.98 (d, $J$ = 2.2 Hz, 1H), 6.84 (dd, $J$ = 8.3, 2.2 Hz, 1H), 5.04 (dd, $J$ = 12.4, 5.4 Hz, 1H), 3.68–3.55 (m, 10H), 3.49 (t, $J$ = 6.2 Hz, 2H), 3.32 (t, $J$ = 6.9 Hz, 2H), 3.11 (t, $J$ = 6.8 Hz, 2H), 2.94–2.62 (m, 3H), 2.16–1.96 (m, 1H), 1.90 (p, $J$ = 6.4 Hz, 2H), 1.70 (p, $J$ = 6.5 Hz, 2H), 1.42 (s, 9H).

**tert-butyl (8-((2-(2,6-dioxopiperidin-3-yl)-1,3-dioxoisoindolin-4-yl)amino)octyl)carbamate(45)** As yellow solids. UPLC-MS:$[M+H]^+$ = 501.39 found. $^1$H NMR (400 MHz, Methanol-$d_4$) δ 7.54 (dd, $J$ = 8.5, 7.2 Hz, 1H), 7.04–6.99 (m, 2H), 5.07 (dd, $J$ = 12.6, 5.4 Hz, 1H), 3.30 (t, $J$ = 6.8 Hz, 3H), 3.03 (t, $J$ = 7.0 Hz, 2H), 2.91–2.67 (m, 3H), 2.26–2.02 (m, 1H), 1.73–1.58 (m, 2H), 1.53–1.24 (m, 19H).

**tert-butyl (9-((2-(2,6-dioxopiperidin-3-yl)-1,3-dioxoisoindolin-4-yl)amino)nonyl)carbamate(46)** As yellow solids. UPLC-MS:$[M+H]^+$ = 515.47 found. $^1$H NMR (400 MHz, Methanol-$d_4$) δ 7.53 (dd, $J$ = 8.4, 7.2 Hz, 1H), 7.05–6.98 (m, 2H), 5.05 (dd, $J$ = 12.6, 5.4 Hz, 1H), 3.30 (t, $J$ = 7.3 Hz, 2H), 3.06–2.97 (m, 2H), 2.93–2.64 (m, 3H), 2.24–1.98 (m, 1H), 1.66 (p, $J$ = 7.1 Hz, 2H), 1.51–1.18 (m, 21H).

**tert-butyl (10-((2-(2,6-dioxopiperidin-3-yl)-1,3-dioxoisoindolin-4-yl)amino)decyl)carbamate(47)** As yellow solids. UPLC-MS:$[M+H]^+$ = 529.40 found. $^1$H NMR (400 MHz, Methanol-$d_4$) δ 7.52 (dd, $J$ = 8.5, 7.1 Hz, 1H), 7.03–6.98 (m, 2H), 5.05 (dd, $J$ = 12.6, 5.4 Hz, 1H), 3.29 (t, $J$ = 6.8 Hz, 2H), 3.01 (t, $J$ = 7.0 Hz, 2H), 2.93–2.65 (m, 3H), 2.15–2.06 (m, 1H), 1.71–1.55 (m, 2H), 1.50–1.23 (m, 23H).

**tert-butyl (11-((2-(2,6-dioxopiperidin-3-yl)-1,3-dioxoisoindolin-4-yl)amino)undecyl)carbamate(48)** As yellow solids. UPLC-MS:$[M+H]^+$ = 543.47 found. $^1$H NMR (400 MHz, Methanol-$d_4$) δ 7.57–7.51 (m, 1H), 7.05–7.00 (m, 2H), 5.05 (dd, $J$ = 12.6, 5.4 Hz, 1H), 3.35–3.28 (m, 2H), 3.07–2.96 (m, 2H), 2.93–2.65 (m, 3H), 2.23–1.98 (m, 1H), 1.66 (p, $J$ = 7.1 Hz, 2H), 1.52–1.19 (m, 25H).

**tert-butyl (12-((2-(2,6-dioxopiperidin-3-yl)-1,3-dioxoisoindolin-4-yl)amino)dodecyl)carbamate(49)** As yellow solids. UPLC-MS:$[M+H]^+$ = 557.60 found. $^1$H NMR (400 MHz, Methanol-$d_4$) δ 7.53 (dd, $J$ = 8.5, 7.1 Hz, 1H), 7.05–6.97 (m, 2H), 5.05 (dd, $J$ = 12.6, 5.4 Hz, 1H), 3.30 (t, $J$ = 7.5 Hz, 2H), 3.01 (t, $J$ = 7.0 Hz, 2H), 2.92–2.64 (m, 3H), 2.16–1.98 (m, 1H), 1.64 (m, 2H), 1.55–1.17 (m, 27H).

**tert-butyl (13-((2-(2,6-dioxopiperidin-3-yl)-1,3-dioxoisoindolin-4-yl)amino)tridecyl)carbamate(50)** As yellow solids. UPLC-MS:$[M+H]^+$ = 571.53 found. $^1$H NMR (400 MHz, Methanol-$d_4$) δ 7.55 (dd, $J$ = 8.5, 7.1 Hz, 1H), 7.06–7.01 (m, 2H), 5.06 (dd, $J$ = 12.5, 5.5 Hz, 1H), 3.35–3.28 (m, 2H), 3.05–2.98 (m, 2H), 2.92–2.65 (m, 3H), 2.31–2.05 (m, 1H), 1.67 (p, $J$ = 7.1 Hz, 2H), 1.48–1.24 (m, 29H).

**N1-(3-((3-amino-5-((3S,4S)-4-amino-3-methyl-2-oxa-8-azaspiro[4.5]decan-8-yl)pyrazin-2-yl)thio)-2-chlorophenyl)-N4-(2-(2-((2-(2,6-dioxopiperidin-3-yl)-1,3-dioxoisoindolin-4-yl) amino)ethoxy)ethyl)succinamide(8)** To a solution of **37** (50 mg, 0.11 mmol) in DCM (10 mL) was added TFA (2 mL), and the mixture was stirred at room temperature for 1 h. After that, the volatiles were removed under reduced pressure and the residual solvents was further evacuated in vacuum.The yellow residue was then dissolved in DMF (5 mL) and to the solution was added **36** (71 mg, 0.11 mmol), HATU (54 mg, 0.14 mmol), DIPEA (90 μL, 0.54 mmol). After stirring at room temperature for 2 h, the mixture was poured into a separating funnel containing sat. aq. $NH_4Cl$ (15 mL) and extracted with EtOAc (10 mL*3). The combined organics were washed with brine and dried over $Na_2SO_4$. Then the volatiles were removed under reduced pressure and the resulting residue was purified by flash chromatography to give the precursor **51** as yellow solids. UPLC-MS:$[M+H]^+$ = 963.53/965.41 found.

To a solution of **51** in DCM (10 mL) was added TFA (2 mL), and the mixture was stirred at room temperature for 1 h. After that, the volatiles were removed under reduced pressure and the residue was dissolved in MeCN and purified by prep-HPLC to give **8** as yellow TFA salts in 52% yield over two steps. UPLC-MS:$[M+H]^+$ = 863.41/865.37 found. $^1$H NMR (400 MHz, DMSO-$d_6$) δ 11.10 (s, 1H), 9.56 (s, 1H), 7.98 (br, 3H), 7.93 (t, $J$ = 5.8 Hz, 1H), 7.66 (s, 1H), 7.58 (t, $J$ = 7.8 Hz, 1H), 7.45 (d, $J$ = 8.0 Hz, 1H), 7.19–7.09 (m, 2H), 7.03 (d, $J$ = 6.5 Hz, 1H), 6.42 (d, $J$ = 8.0 Hz, 1H), 5.05 (dd, $J$ = 12.9,

5.4 Hz, 1H), 4.25–4.07 (m, 3H), 3.88 (d, $J$ = 9.2 Hz, 1H), 3.68 (d, $J$ = 9.1 Hz, 1H), 3.60 (t, $J$ = 5.4 Hz, 2H), 3.51–3.35 (m, 5H), 3.23 (q, $J$ = 5.7 Hz, 2H), 3.11–2.98 (m, 2H), 2.85 (ddd, $J$ = 18.2, 13.8, 6.2 Hz, 1H), 2.66–2.45 (m, 4H), 2.42 (t, $J$ = 7.2 Hz, 2H), 2.08–1.92 (m, 1H), 1.80–1.63 (m, 3H), 1.55 (d, $J$ = 13.1 Hz, 1H), 1.21 (d, $J$ = 7.1 Hz, 3H). $^{13}$C NMR (151 MHz, DMSO-$d_6$) δ 172.93, 171.47, 171.05, 170.20, 169.06, 167.40, 155.91, 153.71, 146.47, 137.40, 136.38, 135.99, 132.14, 129.73, 127.03, 123.28, 122.40, 122.15, 120.38, 117.54, 113.28, 110.81, 109.33, 74.40, 73.39, 69.01, 68.64, 60.64, 48.64, 44.81, 41.70, 41.42, 40.98, 38.63, 33.79, 31.05, 30.40, 22.23, 14.96.

The other PROTAC molecules **9** to **21** were prepared following the same procedures described for the synthesis of **8** in 40%–64% yields.

**N1-(3-((3-amino-5-((3S,4S)-4-amino-3-methyl-2-oxa-8-azaspiro[4.5]decan-8-yl)pyrazin-2-yl)thio)-2-chlorophenyl)-N4-(2-(2-(2-((2-(2,6-dioxopiperidin-3-yl)-1,3-dioxoisoindolin-4-yl)amino)ethoxy)ethoxy)ethyl)succinamide(9)** As yellow TFA salts, UPLC-MS:$[M+H]^+$ = 907.66/909.45 found. $^1$H NMR (400 MHz, DMSO-$d_6$) δ 11.10 (s, 1H), 9.56 (s, 1H), 8.01 (br, 3H), 7.94 (t, $J$ = 5.6 Hz, 1H), 7.66 (s, 1H), 7.56 (dd, $J$ = 8.4, 7.2 Hz, 1H), 7.46 (d, $J$ = 7.9 Hz, 1H), 7.18–7.09 (m, 2H), 7.03 (d, $J$ = 7.1 Hz, 1H), 6.43 (d, $J$ = 7.9 Hz, 1H), 5.05 (dd, $J$ = 13.0, 5.5 Hz, 1H), 4.26–4.06 (m, 3H), 3.88 (d, $J$ = 9.0 Hz, 1H), 3.68 (d, $J$ = 9.1 Hz, 1H), 3.61 (t, $J$ = 5.4 Hz, 2H), 3.58–3.49 (m, 4H), 3.46 (t, $J$ = 5.4 Hz, 2H), 3.43–3.35 (m, 3H), 3.20 (q, $J$ = 5.8 Hz, 2H), 3.12–2.97 (m, 2H), 2.87 (ddd, $J$ = 17.4, 13.9, 5.4 Hz, 1H), 2.66–2.44 (m, 4H), 2.41 (t, $J$ = 7.2 Hz, 2H), 2.08–1.96 (m, 1H), 1.78–1.62 (m, 3H), 1.56 (d, $J$ = 13.0 Hz, 1H), 1.21 (d, $J$ = 6.3 Hz, 3H).$^{13}$C NMR (151 MHz, DMSO-$d_6$) δ 173.04, 171.55, 171.14, 170.30, 169.13, 167.49, 156.04, 153.82, 146.56, 137.42, 136.41, 136.10, 132.24, 129.81, 127.12, 123.38, 122.52, 122.27, 120.35, 117.59, 113.16, 110.87, 109.40, 74.51, 73.47, 69.85, 69.76, 69.30, 69.03, 60.75, 48.74, 44.90, 41.86, 41.52, 41.09, 38.80, 33.89, 31.15, 30.52, 22.32, 15.02.

**N1-(3-((3-amino-5-((3S,4S)-4-amino-3-methyl-2-oxa-8-azaspiro[4.5]decan-8-yl)pyrazin-2-yl)thio)-2-chlorophenyl)-N4-(2-(2-(2-(2-((2-(2,6-dioxopiperidin-3-yl)-1,3-dioxoisoindolin-4-yl)amino)ethoxy)ethoxy)ethoxy)ethyl)succinamide(10)** As yellow TFA salts, UPLC-MS:$[M+H]^+$ = 951.61/953.44 found. $^1$H NMR (400 MHz, DMSO-$d_6$) δ 11.10 (s, 1H), 9.56 (s, 1H), 8.00 (br, 3H), 7.95 (t, $J$ = 5.8 Hz, 1H), 7.65 (s, 1H), 7.57 (dd, $J$ = 8.4, 7.2 Hz, 1H), 7.46 (d, $J$ = 7.9 Hz, 1H), 7.17–7.09 (m, 2H), 7.03 (d, $J$ = 7.0 Hz, 1H), 6.43 (d, $J$ = 7.9 Hz, 1H), 5.04 (dd, $J$ = 12.9, 5.4 Hz, 1H), 4.53–4.04 (m, 3H), 3.88 (d, $J$ = 9.0 Hz, 1H), 3.68 (d, $J$ = 9.1 Hz, 1H), 3.61 (t, $J$ = 5.3 Hz, 2H), 3.58–3.42 (m, 10H), 3.41–3.35 (m, 3H), 3.19 (q, $J$ = 5.8 Hz, 2H), 3.10–2.98 (m, 2H), 2.87 (ddd, $J$ = 17.8, 14.4, 5.3 Hz, 1H), 2.65–2.44 (m, 4H), 2.41 (t, $J$ = 7.2 Hz, 2H), 2.07–1.91 (m, 1H), 1.77–1.64 (m, 3H), 1.55 (d, $J$ = 12.9 Hz, 1H), 1.21 (d, $J$ = 6.6 Hz, 3H). $^{13}$C NMR (151 MHz, DMSO-$d_6$) δ 173.03, 171.54, 171.11, 170.26, 169.09, 167.47, 155.99, 153.79, 146.54, 137.41, 136.40, 136.06, 132.21, 129.79, 127.10, 123.37, 122.51, 122.24, 120.37, 117.59, 113.20, 110.86, 109.35, 74.47, 73.44, 69.92, 69.73, 69.21, 69.01, 60.73, 48.71, 44.87, 41.83, 41.49, 41.05, 38.77, 33.87, 31.12, 30.49, 22.30, 15.00.

**N1-(3-((3-amino-5-((3S,4S)-4-amino-3-methyl-2-oxa-8-azaspiro[4.5]decan-8-yl)pyrazin-2-yl)thio)-2-chlorophenyl)-N4-(3-(2-(2-(3-((2-(2,6-dioxopiperidin-3-yl)-1,3-dioxoisoindolin-4-yl)amino)propoxy)ethoxy)ethoxy)propyl) succinamide(11)** As yellow TFA salts, UPLC-MS:$[M+H]^+$ = 979.72/981.41 found. $^1$H NMR (400 MHz, DMSO-$d_6$) δ 11.11 (s, 1H), 9.57 (s, 1H), 7.99 (s, 3H), 7.87 (t, $J$ = 5.7 Hz, 1H), 7.66 (s, 1H), 7.57 (dd, $J$ = 8.6, 7.1 Hz, 1H), 7.46 (d, $J$ = 7.9 Hz, 1H), 7.14 (t, $J$ = 8.0 Hz, 1H), 7.09 (d, $J$ = 8.6 Hz, 1H), 7.01 (d, $J$ = 7.1 Hz, 1H), 6.68 (s, 1H), 6.41 (d, $J$ = 7.9 Hz, 1H), 5.05 (dd, $J$ = 12.9, 5.4 Hz, 1H), 4.32–4.06 (m, 3H), 3.88 (d, $J$ = 9.0 Hz, 1H), 3.68 (d, $J$ = 9.1 Hz, 1H), 3.58–3.31 (m, 15H), 3.13–2.98 (m, 4H), 2.88 (ddd, $J$ = 17.3, 14.0, 5.4 Hz, 1H), 2.67–2.43 (m, 4H), 2.39 (t, $J$ = 7.2 Hz, 2H), 2.07–1.95 (m, 1H), 1.80 (p, $J$ = 6.4 Hz, 2H), 1.75–1.64 (m, 3H), 1.65–1.51 (m, 3H), 1.21 (d, $J$ = 6.6 Hz, 3H). $^{13}$C NMR (151 MHz, DMSO-$d_6$) δ 172.86, 171.06, 170.95, 170.14, 168.86, 167.35, 155.85, 153.64, 146.45, 137.39, 136.31, 135.96, 132.21, 126.95, 123.21, 122.31, 122.05, 120.35, 117.11, 113.31, 110.39, 109.06, 74.34, 73.33, 69.81, 69.76, 69.72, 69.56, 68.24, 68.08, 60.55, 48.54, 44.76, 41.36, 40.92, 35.87, 33.72, 31.01, 30.46, 29.40, 22.19, 14.93.

**N1-(3-((3-amino-5-((1R,2R)-1-amino-2-methyl-8-azaspiro[4.5]decan-8-yl)pyrazin-2-yl)thio)-2-chlorophenyl)-N4-(2-(2-((2-(2,6-dioxopiperidin-3-yl)-1,3-dioxoisoindolin-5-yl)amino) ethoxy)ethyl)succinamide(12)** As yellow TFA salts, UPLC-MS:$[M+H]^+$ = 863.37/865.17 found. $^1$H NMR (400 MHz, DMSO-$d_6$) δ 11.07 (s, 1H), 9.57 (s, 1H), 8.05 (br, 3H), 7.98 (t, $J$ = 5.6 Hz, 1H), 7.66 (s, 1H), 7.56 (d, $J$ = 8.4 Hz, 1H), 7.46 (d, $J$ = 7.9 Hz, 1H), 7.14 (t, $J$ = 8.0 Hz, 1H), 7.01 (d, $J$ = 2.0 Hz, 1H), 6.90 (dd, $J$ = 8.4, 2.1 Hz, 1H), 6.42 (d, $J$ = 7.8 Hz, 1H), 6.14 (s, 2H), 5.03 (dd, $J$ = 12.9, 5.4 Hz, 1H), 4.29–4.06 (m, 3H), 3.89 (d, $J$ = 9.0 Hz, 1H), 3.68 (d, $J$ = 9.0 Hz, 1H), 3.59 (t, $J$ = 5.4 Hz, 2H), 3.49–3.31 (m, 5H), 3.24 (q, $J$ = 5.7 Hz, 2H), 3.12–2.96 (m, 2H), 2.87 (ddd, $J$ = 17.4, 13.9, 5.4 Hz, 1H), 2.67–2.44 (m, 4H), 2.42 (t, $J$ = 7.2 Hz, 2H), 2.08–1.93 (m, 1H), 1.81–1.63 (m, 3H), 1.56 (d, $J$ = 12.9 Hz, 1H), 1.21 (d, $J$ = 6.4 Hz, 3H). $^{13}$C NMR (126 MHz, DMSO-$d_6$) δ 172.84, 171.41, 170.95, 170.19, 167.71, 167.18, 155.80, 154.43, 153.64, 137.36, 135.94, 134.18, 129.67, 126.95, 125.08, 123.32, 122.38, 122.20, 120.38, 116.19, 113.42, 74.36, 73.27, 69.08, 68.35, 60.57, 48.67, 44.74, 42.45, 41.35, 40.94, 38.54, 33.72, 31.01, 30.41, 22.26, 14.92.

**N1-(3-((3-amino-5-((1R,2R)-1-amino-2-methyl-8-azaspiro[4.5]decan-8-yl)pyrazin-2-yl)thio)-2-chlorophenyl)-N4-(2-(2-(2-((2-(2,6-dioxopiperidin-3-yl)-1,3-dioxoisoindolin-5-yl) amino)ethoxy)ethoxy)ethyl)succinamide(13)** As yellow TFA salts, UPLC-MS:$[M+H]^+$ = 907.24/908.95 found. $^1$H NMR (400 MHz, DMSO-$d_6$) δ 11.07 (s, 1H), 9.56 (s, 1H), 8.04–7.93 (m, 4H), 7.66 (s, 1H), 7.55 (d, $J$ = 8.4 Hz, 1H), 7.45 (d, $J$ = 7.9 Hz, 1H), 7.14 (t, $J$ = 8.0 Hz, 1H), 7.00 (d, $J$ = 2.1 Hz, 1H), 6.89 (dd, $J$ = 8.5, 2.1 Hz, 1H), 6.42 (d, $J$ = 7.9 Hz, 1H), 5.02 (dd, $J$ = 12.9, 5.4 Hz, 1H), 4.38–3.98 (m, 3H), 3.88 (d, $J$ = 9.1 Hz, 1H), 3.68 (d, $J$ = 9.1 Hz, 1H), 3.65–3.48 (m, 6H), 3.43–3.32 (m, 5H), 3.19 (q, $J$ = 5.8 Hz, 2H), 3.11–2.97 (m, 2H), 2.86 (ddd, $J$ = 17.5, 14.1, 5.5 Hz, 1H), 2.65–2.42 (m, 4H), 2.41 (t, $J$ = 7.2 Hz, 2H), 2.04–1.94 (m, 1H), 1.79–1.63 (m, 3H), 1.55 (d, $J$ = 12.9 Hz, 1H), 1.21 (d, $J$ = 6.8 Hz, 3H). $^{13}$C NMR (126 MHz, DMSO-$d_6$) δ 172.88, 171.40, 171.00, 170.22, 167.74, 167.21, 155.85, 154.48, 153.68, 137.35, 135.98, 134.21, 129.70, 126.99, 125.10, 123.34, 122.41, 122.21, 120.36, 116.16, 113.35, 74.37, 73.36, 69.78, 69.62, 69.16, 68.76, 60.63, 48.69, 44.78, 42.52, 41.40, 40.97, 38.66, 33.77, 31.04, 30.41, 22.29, 14.92.

**N1-(3-((3-amino-5-((1R,2R)-1-amino-2-methyl-8-azaspiro[4.5]decan-8-yl)pyrazin-2-yl)thio)-2-chlorophenyl)-N4-(2-(2-(2-(2-((2-(2,6-dioxopiperidin-3-yl)-1,3-dioxoisoindolin-5-yl) amino)ethoxy)ethoxy)ethoxy)ethyl)succinamide(14)** As yellow TFA salts, UPLC-MS:$[M+H]^+$ = 951.19/953.40 found. $^1$H NMR (400 MHz, DMSO-$d_6$) δ 11.07 (s, 1H), 9.56 (s, 1H), 8.03–7.93 (m, 4H), 7.66 (s, 1H), 7.55 (d, $J$ = 8.3 Hz, 1H), 7.46 (d, $J$ = 7.9 Hz, 1H), 7.14 (t, $J$ = 8.1 Hz, 1H), 7.00 (d, $J$ = 2.1 Hz, 1H), 6.89 (dd, $J$ = 8.4, 2.1 Hz, 1H), 6.42 (d, $J$ = 7.8 Hz, 1H), 5.03 (dd, $J$ = 12.9, 5.4 Hz, 1H), 4.29–4.01 (m, 3H), 3.88 (d, $J$ = 9.1 Hz, 1H), 3.68 (d, $J$ = 9.1 Hz, 1H), 3.59 (t, $J$ = 5.4 Hz, 2H), 3.57–3.46 (m, 8H), 3.37 (dt, $J$ = 13.6, 5.7 Hz, 5H), 3.19 (q, $J$ = 5.8 Hz, 2H), 3.12–2.97 (m, 2H), 2.94–2.80 (m, 1H), 2.65–2.43 (m, 4H), 2.41 (t, $J$ = 7.2 Hz, 2H), 2.04–1.93 (m, 1H), 1.77–1.63 (m, 3H), 1.55 (d, $J$ = 13.4 Hz, 1H), 1.21 (d, $J$ = 7.4 Hz, 3H). $^{13}$C NMR (126 MHz, DMSO-$d_6$) δ 172.83, 171.32, 170.94, 170.17, 167.70, 167.16, 155.81, 154.45, 153.64, 137.33, 135.95, 134.17, 129.66, 126.95, 125.05, 123.29, 122.36, 122.17, 120.34, 116.11, 113.37, 74.34, 73.33, 69.80, 69.76, 69.59, 69.10, 68.74, 60.58, 48.65, 44.74, 42.47, 41.36, 40.93, 38.63, 33.73, 31.00, 30.38, 22.26, 14.89.

**N1-(3-((3-amino-5-((1R,2R)-1-amino-2-methyl-8-azaspiro[4.5]decan-8-yl)pyrazin-2-yl)thio)-2-chlorophenyl)-N4-(3-(2-(2-(3-((2-(2,6-dioxopiperidin-3-yl)-1,3-dioxoisoindolin-5-yl) amino)propoxy)ethoxy)ethoxy)propyl)succinamide(15)** As

yellow TFA salts, UPLC-MS:$[M+H]^+$ = 979.72/981.41 found. $^1$H NMR (400 MHz, DMSO-$d_6$) δ 11.07 (s, 1H), 9.57 (s, 1H), 8.01 (s, 3H), 7.87 (t, $J$ = 5.6 Hz, 1H), 7.65 (s, 1H), 7.55 (d, $J$ = 8.3 Hz, 1H), 7.45 (d, $J$ = 7.9 Hz, 1H), 7.14 (t, $J$ = 8.0 Hz, 1H), 6.94 (d, $J$ = 2.1 Hz, 1H), 6.84 (dd, $J$ = 8.4, 2.2 Hz, 1H), 6.42 (dd, $J$ = 7.9, 1.5 Hz, 1H), 6.13 (s, 2H), 5.02 (dd, $J$ = 12.9, 5.4 Hz, 1H), 4.27–4.06 (m, 3H), 3.88 (d, $J$ = 9.1 Hz, 1H), 3.68 (d, $J$ = 9.1 Hz, 1H), 3.56–3.33 (m, 10H), 3.21 (q, $J$ = 6.1 Hz, 2H), 3.13–2.97 (m, 4H), 2.86 (ddd, $J$ = 17.5, 14.0, 5.4 Hz, 1H), 2.65–2.42 (m, 4H), 2.39 (t, $J$ = 7.2 Hz, 2H), 2.06–1.92 (m, 2H), 1.77 (q, $J$ = 6.5 Hz, 2H), 1.74–1.49 (m, 6H), 1.21 (d, $J$ = 7.0 Hz, 3H). $^{13}$C NMR (151 MHz, DMSO-$d_6$) δ 172.94, 171.18, 171.01, 170.26, 167.75, 167.23, 155.86, 154.52, 153.67, 137.40, 135.96, 134.23, 129.71, 127.00, 125.20, 123.28, 122.40, 122.13, 120.40, 115.93, 113.34, 74.38, 73.32, 69.83, 69.82, 69.65, 69.59, 68.11, 67.81, 60.61, 48.67, 44.78, 41.38, 40.94, 35.92, 33.76, 31.04, 30.50, 29.40, 22.30, 14.95.

**N1-(3-((3-amino-5-((1R,2R)-1-amino-2-methyl-8-azaspiro [4.5]decan-8-yl)pyrazin-2-yl)thio)-2-chlorophenyl)-N4-(8-((2-(2,6-dioxopiperidin-3-yl)-1,3-dioxoisoindolin-4-yl)amino)octyl) succinamide(16)** As yellow TFA salts, UPLC-MS:$[M+H]^+$ = 903.64/905.38 found. $^1$H NMR (400 MHz, DMSO-$d_6$) δ 11.10 (s, 1H), 9.56 (s, 1H), 7.99 (br, 3H), 7.85 (t, $J$ = 5.6 Hz, 1H), 7.66 (s, 1H), 7.57 (dd, $J$ = 8.6, 7.1 Hz, 1H), 7.46 (d, $J$ = 7.9 Hz, 1H), 7.14 (t, $J$ = 8.1 Hz, 1H), 7.08 (d, $J$ = 8.6 Hz, 1H), 7.01 (d, $J$ = 7.0 Hz, 1H), 6.44–6.40 (m, 1H), 5.05 (dd, $J$ = 12.9, 5.4 Hz, 1H), 4.29–4.07 (m, 3H), 3.88 (d, $J$ = 9.1 Hz, 1H), 3.68 (d, $J$ = 9.0 Hz, 1H), 3.40 (t, $J$ = 5.3 Hz, 1H), 3.28 (t, $J$ = 7.1 Hz, 2H), 3.13–2.97 (m, 4H), 2.95–2.80 (m, 1H), 2.66–2.43 (m, 4H), 2.39 (t, $J$ = 7.2 Hz, 2H), 2.08–1.92 (m, 1H), 1.77–1.63 (m, 3H), 1.63–1.49 (m, 3H), 1.43–1.12 (m, 13H). $^{13}$C NMR (126 MHz, DMSO-$d_6$) δ 172.78, 170.92, 170.07, 168.94, 167.29, 155.77, 153.61, 146.43, 137.31, 136.26, 135.94, 132.17, 129.63, 126.90, 122.27, 122.11, 120.32, 117.16, 113.36, 110.36, 109.00, 74.31, 73.31, 60.54, 48.55, 44.72, 41.85, 41.34, 40.90, 38.52, 33.70, 30.98, 30.49, 29.10, 28.71, 28.68, 26.35, 26.29, 22.16, 14.89.

**N1-(3-((3-amino-5-((1R,2R)-1-amino-2-methyl-8-azaspiro [4.5]decan-8-yl)pyrazin-2-yl)thio)-2-chlorophenyl)-N4-(9-((2-(2,6-dioxopiperidin-3-yl)-1,3-dioxoisoindolin-4-yl)amino) nonyl)succinamide(17)** As yellow TFA salts, UPLC-MS:$[M+H]^+$ = 917.66/919.40 found. $^1$H NMR (400 MHz, DMSO-$d_6$) δ 11.10 (s, 1H), 9.56 (s, 1H), 8.03 (br, 3H), 7.85 (t, $J$ = 5.6 Hz, 1H), 7.65 (s, 1H), 7.56 (dd, $J$ = 8.0, 7.6 Hz, 1H), 7.47 (d, $J$ = 7.9 Hz, 1H), 7.13 (t, $J$ = 8.0 Hz, 1H), 7.07 (d, $J$ = 8.6 Hz, 1H), 7.01 (d, $J$ = 7.0 Hz, 1H), 6.42 (d, $J$ = 7.9 Hz, 1H), 5.05 (dd, $J$ = 12.9, 5.4 Hz, 1H), 4.27–4.06 (m, 3H), 3.88 (d, $J$ = 9.2 Hz, 1H), 3.68 (d, $J$ = 9.1 Hz, 1H), 3.40 (t, $J$ = 5.4 Hz, 1H), 3.27 (t, $J$ = 7.1 Hz, 2H), 3.12–2.95 (m, 4H), 2.95–2.81 (m, 1H), 2.67–2.44 (m, 4H), 2.39 (t, $J$ = 7.2 Hz, 2H), 2.07–1.93 (m, 1H), 1.78–1.62 (m, 3H), 1.62–1.48 (m, 3H), 1.42–1.12 (m, 15H). $^{13}$C NMR (126 MHz, DMSO-$d_6$) δ 172.83, 170.98, 170.11, 168.97, 167.32, 155.80, 153.63, 146.44, 137.34, 136.28, 135.95, 132.18, 129.65, 126.93, 123.21, 122.26, 122.10, 120.34, 117.17, 113.34, 110.39, 109.00, 74.35, 73.27, 60.55, 48.56, 44.73, 41.86, 41.34, 40.91, 38.56, 33.71, 31.00, 30.51, 29.14, 28.97, 28.73, 28.70, 26.40, 26.33, 22.18, 14.90.

**N1-(3-((3-amino-5-((1R,2R)-1-amino-2-methyl-8-azaspiro [4.5]decan-8-yl)pyrazin-2-yl)thio)-2-chlorophenyl)-N4-(10-((2-(2,6-dioxopiperidin-3-yl)-1,3-dioxoisoindolin-4-yl)amino) decyl)succinamide(18)** As yellow TFA salts, UPLC-MS:$[M+H]^+$ = 931.64/933.43 found. $^1$H NMR (400 MHz, DMSO-$d_6$) δ 11.10 (s, 1H), 9.56 (s, 1H), 8.00 (br, 3H), 7.85 (t, $J$ = 5.6 Hz, 1H), 7.66 (s, 1H), 7.56 (dd, $J$ = 8.6, 7.1 Hz, 1H), 7.47 (d, $J$ = 7.9 Hz, 1H), 7.14 (t, $J$ = 8.0 Hz, 1H), 7.06 (d, $J$ = 8.6 Hz, 1H), 7.01 (d, $J$ = 7.0 Hz, 1H), 6.43 (dd, $J$ = 8.0, 1.4 Hz, 1H), 5.05 (dd, $J$ = 12.9, 5.4 Hz, 1H), 4.27–4.06 (m, 3H), 3.88 (d, $J$ = 9.0 Hz, 1H), 3.68 (d, $J$ = 9.1 Hz, 1H), 3.40 (t, $J$ = 5.3 Hz, 1H), 3.27 (t, $J$ = 7.1 Hz, 2H), 3.12–2.96 (m, 4H), 2.95–2.81 (m, 1H), 2.68–2.44 (m, 4H), 2.39 (t, $J$ = 7.2 Hz, 2H), 2.09–1.94 (m, 1H), 1.80–1.62 (m, 3H), 1.62–1.49 (m, 3H), 1.45–1.12 (m, 17H). $^{13}$C NMR (126 MHz, DMSO-$d_6$) δ 172.83, 171.00, 170.11, 169.01, 167.35, 155.86, 153.68, 146.49, 137.32, 136.28, 136.01, 132.23, 129.66, 126.95, 123.26, 122.30, 122.17, 120.29, 117.17, 113.30, 110.41, 109.07, 74.38, 73.36, 60.61, 48.61, 44.77, 41.91, 41.41, 40.97, 38.60, 33.77, 31.04, 30.55, 29.18, 29.00, 28.80, 28.73, 26.45, 26.37, 22.22, 14.91.

**N1-(3-((3-amino-5-((1R,2R)-1-amino-2-methyl-8-azaspiro [4.5]decan-8-yl)pyrazin-2-yl)thio)-2-chlorophenyl)-N4-(11-((2-(2,6-dioxopiperidin-3-yl)-1,3-dioxoisoindolin-4-yl)amino) undecyl)succinamide(19)** As yellow TFA salts, UPLC-MS:$[M+H]^+$ = 945.71/947.46 found. $^1$H NMR (400 MHz, DMSO-$d_6$) δ 11.10 (s, 1H), 9.56 (s, 1H), 8.02 (br, 3H), 7.85 (t, $J$ = 5.6 Hz, 1H), 7.65 (s, 1H), 7.56 (dd, $J$ = 8.5, 7.1 Hz, 1H), 7.46 (d, $J$ = 7.9 Hz, 1H), 7.13 (t, $J$ = 8.0 Hz, 1H), 7.07 (d, $J$ = 8.6 Hz, 1H), 7.01 (d, $J$ = 7.0 Hz, 1H), 6.42 (d, $J$ = 7.8 Hz, 1H), 5.04 (dd, $J$ = 12.9, 5.4 Hz, 1H), 4.26–4.06 (m, 3H), 3.88 (d, $J$ = 9.1 Hz, 1H), 3.67 (d, $J$ = 9.1 Hz, 1H), 3.39 (t, $J$ = 5.3 Hz, 1H), 3.27 (t, $J$ = 7.1 Hz, 2H), 3.10–2.97 (m, 4H), 2.88 (ddd, $J$ = 17.4, 14.0, 5.4 Hz, 1H), 2.65–2.43 (m, 4H), 2.39 (t, $J$ = 7.2 Hz, 2H), 2.09–1.91 (m, 1H), 1.80–1.63 (m, 3H), 1.62–1.49 (m, 3H), 1.42–1.15 (m, 19H). $^{13}$C NMR (126 MHz, DMSO-$d_6$) δ 172.87, 171.01, 170.13, 169.00, 167.36, 155.83, 153.66, 146.48, 137.37, 136.32, 135.98, 132.21, 129.68, 126.96, 123.25, 122.31, 122.14, 120.38, 117.21, 113.39, 110.42, 109.02, 74.37, 73.31, 60.59, 48.59, 44.76, 41.88, 41.37, 40.94, 38.60, 33.75, 31.02, 30.53, 29.17, 29.04, 28.81, 28.72, 26.46, 26.36, 22.21, 14.93.

**N1-(3-((3-amino-5-((1R,2R)-1-amino-2-methyl-8-azaspiro [4.5]decan-8-yl)pyrazin-2-yl)thio)-2-chlorophenyl)-N4-(12-((2-(2,6-dioxopiperidin-3-yl)-1,3-dioxoisoindolin-4-yl)amino) dodecyl)succinamide(20)** As yellow TFA salts, UPLC-MS:$[M+H]^+$ = 959.79/961.48 found. $^1$H NMR (400 MHz, DMSO-$d_6$) δ 11.10 (s, 1H), 9.56 (s, 1H), 8.01 (br, 3H), 7.85 (t, $J$ = 5.6 Hz, 1H), 7.66 (s, 1H), 7.56 (dd, $J$ = 8.6, 7.0 Hz, 1H), 7.47 (d, $J$ = 8.0 Hz, 1H), 7.14 (t, $J$ = 8.0 Hz, 1H), 7.07 (d, $J$ = 8.6 Hz, 1H), 7.01 (d, $J$ = 7.0 Hz, 1H), 6.43 (dd, $J$ = 8.0, 1.5 Hz, 1H), 5.05 (dd, $J$ = 12.9, 5.4 Hz, 1H), 4.25–4.07 (m, 3H), 3.88 (d, $J$ = 9.0 Hz, 1H), 3.68 (d, $J$ = 9.1 Hz, 1H), 3.40 (t, $J$ = 5.3 Hz, 1H), 3.27 (t, $J$ = 7.1 Hz, 2H), 3.12–2.95 (m, 4H), 2.88 (ddd, $J$ = 17.5, 14.0, 5.4 Hz, 1H), 2.66–2.44 (m, 4H), 2.39 (t, $J$ = 7.2 Hz, 2H), 2.09–1.93 (m, 1H), 1.79–1.61 (m, $J$ = 5.1, 4.1 Hz, 3H), 1.61–1.50 (m, 3H), 1.42–1.14 (m, 21H). $^{13}$C NMR (126 MHz, DMSO-$d_6$) δ 172.81, 170.98, 170.09, 168.99, 167.33, 155.82, 153.66, 146.47, 137.32, 136.27, 135.99, 132.21, 129.65, 126.93, 123.25, 122.29, 122.15, 120.30, 117.16, 113.33, 110.39, 109.05, 74.36, 73.33, 60.59, 48.59, 44.76, 41.88, 41.38, 40.95, 38.59, 33.75, 31.02, 30.53, 29.16, 29.03, 28.80, 28.79, 28.71, 26.45, 26.34, 22.20, 14.90.

**N1-(3-((3-amino-5-((1R,2R)-1-amino-2-methyl-8-azaspiro [4.5]decan-8-yl)pyrazin-2-yl)thio)-2-chlorophenyl)-N4-(13-((2-(2,6-dioxopiperidin-3-yl)-1,3-dioxoisoindolin-4-yl)amino)tri-decyl)succinamide(21)** As yellow TFA salts, UPLC-MS:$[M+H]^+$ = 973.77/975.46 found. $^1$H NMR (400 MHz, DMSO-$d_6$) δ 11.10 (s, 1H), 9.56 (s, 1H), 7.96 (br, 3H), 7.85 (t, $J$ = 5.6 Hz, 1H), 7.65 (s, 1H), 7.57 (t, $J$ = 7.8 Hz, 1H), 7.46 (d, $J$ = 8.0 Hz, 1H), 7.13 (t, $J$ = 8.1 Hz, 1H), 7.08 (d, $J$ = 8.6 Hz, 1H), 7.01 (d, $J$ = 7.0 Hz, 1H), 6.42 (d, $J$ = 8.0 Hz, 1H), 5.04 (dd, $J$ = 12.8, 5.4 Hz, 1H), 4.28–4.05 (m, 3H), 3.88 (d, $J$ = 9.0 Hz, 1H), 3.68 (d, $J$ = 9.1 Hz, 1H), 3.56–3.19 (m, 3H), 3.13–2.95 (m, 4H), 2.97–2.80 (m, 1H), 2.65–2.44 (m, 4H), 2.38 (t, $J$ = 7.3 Hz, 2H), 2.08–1.89 (m, 1H), 1.79–1.62 (m, 3H), 1.62–1.49 (m, 3H), 1.48–1.11 (m, 23H). $^{13}$C NMR (126 MHz, DMSO-$d_6$) δ 172.85, 171.00, 170.11, 168.99, 167.34, 155.80, 153.65, 146.48, 137.35, 136.32, 135.97, 132.20, 129.68, 126.95, 123.29, 122.32, 122.17, 120.39, 117.22, 113.45, 110.43, 109.02, 74.36, 73.35, 60.61, 48.59, 44.76, 41.88, 41.39, 40.94, 38.59, 33.75, 31.01, 30.53, 29.03, 28.80, 28.78, 26.44, 26.33, 22.20, 14.93.

### 5.2. Cell line and cell culture

The biphenotypic B myelomonocytic leukemia cell line MV4; 11 was obtained from the American Type Culture Collection (ATCC) (Manassas, VA, USA). MV4; 11 cells were maintained at 37 °C in

Iscove's Modified Dulbecco's medium supplemented with 10% fetal bovine serum (FBS) (GIBCO), 100 U/mL penicillin, and 100 μg/mL streptomycin (Invitrogen, USA). Cells were cultured according to the provider's instructions and maintained at 37 °C in a humidified atmosphere containing 5% $CO_2$ in air. Also, MV4; 11 cell line was authenticated using STR profiling (Shanghai Genesky Biotechnology Co., Ltd.).

### 5.3. Western blotting analysis

For Western blotting analysis, $1.0 \times 10^6$ cells/well were plated in 6-well plates, then treated with individual compound at indicated concentrations for a specific period of time. After that cells were washed with ice-cold PBS and lysed with RIPA buffer containing protease inhibitors for 30 min.

Equal amounts of protein were separated using SDS-PAGE and subsequently transferred onto a nitrocellulose membrane. The membranes were blocked with TBST buffer with 5% nonfat dry milk and incubated with primary anti-human antibody followed by secondary antibody. Software ImageJ was used to quantify the percentage of SHP2 degradation.

### 5.4. Cell growth assay

Cells were seeded in 96-well cell culture plates at a density of $1.0–4.0 \times 10^4$ cells/well in 80 μL of culture medium. After 2 h of incubation, the cells were treated with 20 μL of 0.01% DMSO or varying concentrations of the test compounds for 72 h at 37 °C in an atmosphere of 5% $CO_2$.

Cell viability was measured using the CellTiter 96® Aqueous non-radioactive cell proliferation assay (MTS; Promega, Madison, WI). The combined solution of MTS/PMS (20 μL) was pipetted into each well of the 96-well plates and incubated at 37 °C for 2–4 h. The $IC_{50}$ values were derived from a nonlinear regression model (curve fit) based on a sigmoidal dose-response curve (variable slope) and computed using GraphPad software. The results are presented as the mean ± SEM from at least three separate assays performed in triplicate.

### 5.5. Cell cycle arrest and apoptosis

For cell cycle analysis, after treatment cells were collected, washed twice with cold PBS, fixed in ethanol overnight at 4 °C, and finally stained with propidium iodide (PI) plus RNase for 15 min at 37 °C. For apoptosis assays, the cells were washed twice with ice-cold PBS after drug treatment. Annexin V-FITC/PI Apoptosis Detection Kit (KeyGen Biotech, Nanjing, China) was used to assess apoptosis according to the manufacturer's instructions. Data were acquired using flow cytometry.

## Declaration of competing interest

The authors declare that they have no known competing financial interests or personal relationships that could have appeared to influence the work reported in this paper.

## Acknowledgment

The authors appreciate the financial support from the National Natural Science Foundation of China (81973166, 21702218, 21772068, 81773779, 81773568, 91753207), the National Science and Technology Major Project of China (2018ZX09711002-008-004, 2018ZX09711002-008-005, 2018ZX09711002-006-001), K. C. Wong Education Foundation, and Youth innovation promotion association (2017333).

## References

[1] R.J. Chan, G.S. Feng, PTPN11 is the first identified proto-oncogene that encodes a tyrosine phosphatase, Blood 109 (2007) 862–867.
[2] X.-F.S. Ighodaro Igbe, Wei Jiao, Zhe Qiang, Teng Deng, Sheng Li, Wan-Li Liu, Han-Wei Liu, Guo-Lin Zhang, Fei Wang, Dietary quercetin potentiates the antiproliferative effect of interferon-α in hepatocellular carcinoma cells through activation of JAK/STAT pathway signaling by inhibition of SHP2 phosphatase, Oncotarget (2017) 113734–113748.
[3] R.P. Zhou, S.J. Lin, W.B. Wan, H.L. Zuo, F.F. Yao, H.B. Ruan, J. Xu, W. Song, Y.C. Zhou, S.Y. Wen, J.H. Dai, M.L. Zhu, J. Luo, Chlorogenic acid prevents osteoporosis by Shp2/PI3K/Akt pathway in ovariectomized rats, PloS One 11 (2016) e0166751.
[4] S. Mainardi, A. Mulero-Sanchez, A. Prahallad, G. Germano, A. Bosma, P. Krimpenfort, C. Lieftink, J.D. Steinberg, N. de Wit, S. Goncalves-Ribeiro, E. Nadal, A. Bardelli, A. Villanueva, R. Bernards, SHP2 is required for growth of KRAS-mutant non-small-cell lung cancer in vivo, Nat. Med. 24 (2018) 961–967.
[5] M. Tartaglia, E.L. Mehler, R. Goldberg, G. Zampino, H.G. Brunner, H. Kremer, I. van der Burgt, A.H. Crosby, A. Ion, S. Jeffery, K. Kalidas, M.A. Patton, R.S. Kucherlapati, B.D. Gelb, Mutations in PTPN11, encoding the protein tyrosine phosphatase SHP-2, cause Noonan syndrome, Nat. Genet. 29 (2001) 465–468.
[6] C.M.N. Marco Tartaglia, Alessandra Fragale, Xiaoling Song, Jochen Buechner, Andreas Jung, Karel Hählen, Henrik Hasle, Jonathan D Licht, Bruce D. Gelb, Somatic mutations in PTPN11 in juvenile myelomonocytic leukemia, myelodysplastic syndromes and acute myeloid leukemia, Nat. Genet. 34 (2003) 148–150.
[7] M.L. Loh, S. Vattikuti, S. Schubbert, M.G. Reynolds, E. Carlson, K.H. Lieuw, J.W. Cheng, C.M. Lee, D. Stokoe, J.M. Bonifas, N.P. Curtiss, J. Gotlib, S. Meshinchi, M.M. Le Beau, P.D. Emanuel, K.M. Shannon, Mutations in PTPN11 implicate the SHP-2 phosphatase in leukemogenesis, Blood 103 (2004) 2325–2331.
[8] D. Miyamoto, M. Miyamoto, A. Takahashi, Y. Yomogita, H. Higashi, S. Kondo, M. Hatakeyama, Isolation of a distinct class of gain-of-function SHP-2 mutants with oncogenic RAS-like transforming activity from solid tumors, Oncogene 27 (2008) 3508–3515.
[9] J. Li, H.B. Jie, Y. Lei, N. Gildener-Leapman, S. Trivedi, T. Green, L.P. Kane, R.L. Ferris, PD-1/SHP-2 inhibits Tc1/Th1 phenotypic responses and the activation of T cells in the tumor microenvironment, Canc. Res. 75 (2015) 508–518.
[10] M.O.A.J.B. Sam Butterworth, Targeting protein tyrosine phosphatase SHP2 for therapeutic intervention, Future Med. Chem. 6 (12) (2014) 1423–1437.
[11] Y.N. Chen, M.J. LaMarche, H.M. Chan, P. Fekkes, J. Garcia-Fortanet, M.G. Acker, B. Antonakos, C.H. Chen, Z. Chen, V.G. Cooke, J.R. Dobson, Z. Deng, F. Fei, B. Firestone, M. Fodor, C. Fridrich, H. Gao, D. Grunenfelder, H.X. Hao, J. Jacob, S. Ho, K. Hsiao, Z.B. Kang, R. Karki, M. Kato, J. Larrow, L.R. La Bonte, F. Lenoir, G. Liu, S. Liu, D. Majumdar, M.J. Meyer, M. Palermo, L. Perez, M. Pu, E. Price, C. Quinn, S. Shakya, M.D. Shultz, J. Slisz, K. Venkatesan, P. Wang, M. Warmuth, S. Williams, G. Yang, J. Yuan, J.H. Zhang, P. Zhu, T. Ramsey, N.J. Keen, W.R. Sellers, T. Stams, P.D. Fortin, Allosteric inhibition of SHP2 phosphatase inhibits cancers driven by receptor tyrosine kinases, Nature 535 (2016) 148–152.
[12] J. Garcia Fortanet, C.H. Chen, Y.N. Chen, Z. Chen, Z. Deng, B. Firestone, P. Fekkes, M. Fodor, P.D. Fortin, C. Fridrich, D. Grunenfelder, S. Ho, Z.B. Kang, R. Karki, M. Kato, N. Keen, L.R. LaBonte, J. Larrow, F. Lenoir, G. Liu, S. Liu, F. Lombardo, D. Majumdar, M.J. Meyer, M. Palermo, L. Perez, M. Pu, T. Ramsey, W.R. Sellers, M.D. Shultz, T. Stams, C. Towler, P. Wang, S.L. Williams, J.H. Zhang, M.J. LaMarche, Allosteric inhibition of SHP2: identification of a potent, selective, and orally efficacious phosphatase inhibitor, J. Med. Chem. 59 (2016) 7773–7782.
[13] P. Sarver, M. Acker, J.T. Bagdanoff, Z. Chen, Y.N. Chen, H. Chan, B. Firestone, M. Fodor, J. Fortanet, H. Hao, M. Hentemann, M. Kato, R. Koenig, L.R. LaBonte, G. Liu, S. Liu, C. Liu, E. McNeill, M. Mohseni, M. Sendzik, T. Stams, S. Spence, V. Tamez, R. Tichkule, C. Towler, H. Wang, P. Wang, S.L. Williams, B. Yu, M.J. LaMarche, 6-Amino-3-methylpyrimidinones as potent, selective, and orally efficacious SHP2 inhibitors, J. Med. Chem. 62 (2019) 1793–1802.
[14] J.T. Bagdanoff, Z. Chen, M. Acker, Y.N. Chen, H. Chan, M. Dore, B. Firestone, M. Fodor, J. Fortanet, M. Hentemann, M. Kato, R. Koenig, L.R. LaBonte, S. Liu, M. Mohseni, R. Ntaganda, P. Sarver, T. Smith, M. Sendzik, T. Stams, S. Spence, C. Towler, H. Wang, P. Wang, S.L. Williams, M.J. LaMarche, Optimization of fused bicyclic allosteric SHP2 inhibitors, J. Med. Chem. 62 (2019) 1781–1792.
[15] M.J. LaMarche, M.G. Acker, A. Argintaru, D. Bauer, J. Boisclair, H. Chan, C. Chen, Y.P. Chen, Z. Chen, Z. Deng, M. Dore, D. Dunstan, J. Fan, P. Fekkes, B. Firestone, M. Fodor, J. Garcia-Fortanet, P.D. Fortin, C. Fridrich, J. Giraldes, M. Glick, D. Grunenfelder, H.X. Hao, M. Hentemann, S. Ho, A. Jouk, Z.B. Kang, R. Karki, M. Kato, N. Keen, R. Koenig, L.R. LaBonte, J. Larrow, G. Liu, S. Liu, D. Majumdar, S. Mathieu, M. Meyer, M. Mohseni, R. Ntaganda, M. Palermo, L.B. Perez, M. Pu, T. Ramsey, J. Reilly, P. Sarver, W.R. Sellers, M. Sendzick, M.D. Shultz, J. Slisz, K. Slocum, T. Smith, S. Spence, T. Stams, C. Straub, V. Tamez, B.B. Toure, C. Towler, P. Wang, H. Wang, S.L. Williams, F. Yang, B. Yu, J.H. Zhang, S. Zhu, Identification of TNO155, an allosteric SHP2 inhibitor for the treatment of cancer, J. Med. Chem. 63 (2020) 13578–13594.
[16] K.B.K. Kathleen, M. Sakamoto, Akiko Kumagai, Frank Mercurio, Craig

M. Crews, Raymond J. Deshaies, Protacs: chimeric molecules that target proteins to the Skp1–Cullin–F box complex for ubiquitination and degradation, Proc. Natl. Acad. Sci. U. S. A. 98 (2001) 8554–8559.
[17] G.M. Burslem, J. Song, X. Chen, J. Hines, C.M. Crews, Enhancing antiproliferative activity and selectivity of a FLT-3 inhibitor by proteolysis targeting chimera conversion, J. Am. Chem. Soc. 140 (2018) 16428–16432.
[18] C.E. Powell, Y. Gao, L. Tan, K.A. Donovan, R.P. Nowak, A. Loehr, M. Bahcall, E.S. Fischer, P.A. Janne, R.E. George, N.S. Gray, Chemically induced degradation of Anaplastic lymphoma kinase (ALK), J. Med. Chem. 61 (2018) 4249–4255.
[19] E.S.W. Dennis Dobrovolsky, Sara Morrow, Catharine Leahy, Tyler Faust, P. Radosław, Nowak, Katherine, A. Donovan, Guang Yang, Li Zhengnian, S. Eric, Fischer, P. Steven, Treon, M. David, Weinstock, S. Nathanael, Gray, Bruton tyrosine kinase degradation as a therapeutic strategy for cancer, Blood 13 (2019) 952–961.
[20] B. Jiang, E.S. Wang, K.A. Donovan, Y. Liang, E.S. Fischer, T. Zhang, N.S. Gray, Development of dual and selective degraders of cyclin-dependent kinases 4 and 6, in: Angew Chem Int (Ed.), Engl, vol. 58, 2019, pp. 6321–6326.
[21] J. Lu, Y. Qian, M. Altieri, H. Dong, J. Wang, K. Raina, J. Hines, J.D. Winkler, A.P. Crew, K. Coleman, C.M. Crews, Hijacking the E3 ubiquitin ligase cereblon to efficiently target BRD4, Chem Biol 22 (2015) 755–763.
[22] K. Raina, J. Lu, Y. Qian, M. Altieri, D. Gordon, A.M. Rossi, J. Wang, X. Chen, H. Dong, K. Siu, J.D. Winkler, A.P. Crew, C.M. Crews, K.G. Coleman, PROTAC-induced BET protein degradation as a therapy for castration-resistant prostate cancer, Proc. Natl. Acad. Sci. U. S. A. 113 (2016) 7124–7129.
[23] C. Qin, Y. Hu, B. Zhou, E. Fernandez-Salas, C.Y. Yang, L. Liu, D. McEachern, S. Przybranowski, M. Wang, J. Stuckey, J. Meagher, L. Bai, Z. Chen, M. Lin, J. Yang, D.N. Ziazadeh, F. Xu, J. Hu, W. Xiang, L. Huang, S. Li, B. Wen, D. Sun, S. Wang, Discovery of QCA570 as an exceptionally potent and efficacious proteolysis targeting chimera (PROTAC) degrader of the bromodomain and extra-terminal (BET) proteins capable of inducing complete and durable tumor regression, J. Med. Chem. 61 (2018) 6685–6704.
[24] M. Schiedel, D. Herp, S. Hammelmann, S. Swyter, A. Lehotzky, D. Robaa, J. Olah, J. Ovadi, W. Sippl, M. Jung, Chemically induced degradation of sirtuin 2 (Sirt2) by a proteolysis targeting chimera (PROTAC) based on sirtuin rearranging ligands (SirReals), J. Med. Chem. 61 (2018) 482–491.
[25] H. Wu, K. Yang, Z. Zhang, E.D. Leisten, Z. Li, H. Xie, J. Liu, K.A. Smith, Z. Novakova, C. Barinka, W. Tang, Development of multifunctional histone deacetylase 6 degraders with potent Antimyeloma activity, J. Med. Chem. 62 (2019) 7042–7057.
[26] X. Han, C. Wang, C. Qin, W. Xiang, E. Fernandez-Salas, C.Y. Yang, M. Wang, L. Zhao, T. Xu, K. Chinnaswamy, J. Delproposto, J. Stuckey, S. Wang, Discovery of ARD-69 as a highly potent proteolysis targeting chimera (PROTAC) degrader of Androgen receptor (AR) for the treatment of prostate cancer, J. Med. Chem. 62 (2019) 941–964.
[27] X. Han, L. Zhao, W. Xiang, C. Qin, B. Miao, T. Xu, M. Wang, C.Y. Yang, K. Chinnaswamy, J. Stuckey, S. Wang, Discovery of highly potent and efficient PROTAC degraders of Androgen receptor (AR) by employing weak binding Affinity VHL E3 ligase ligands, J. Med. Chem. 62 (2019) 11218–11231.
[28] J. Hu, B. Hu, M. Wang, F. Xu, B. Miao, C.Y. Yang, M. Wang, Z. Liu, D.F. Hayes, K. Chinnaswamy, J. Delproposto, J. Stuckey, S. Wang, Discovery of ERD-308 as a highly potent proteolysis targeting chimera (PROTAC) degrader of estrogen receptor (ER), J. Med. Chem. 62 (2019) 1420–1442.
[29] H. Zhou, L. Bai, R. Xu, Y. Zhao, J. Chen, D. McEachern, K. Chinnaswamy, B. Wen, L. Dai, P. Kumar, C.Y. Yang, Z. Liu, M. Wang, L. Liu, J.L. Meagher, H. Yi, D. Sun, J.A. Stuckey, S. Wang, Structure-based discovery of SD-36 as a potent, selective, and efficacious PROTAC degrader of STAT3 protein, J. Med. Chem. 62 (2019) 11280–11300.
[30] L. Bai, H. Zhou, R. Xu, Y. Zhao, K. Chinnaswamy, D. McEachern, J. Chen, C.Y. Yang, Z. Liu, M. Wang, L. Liu, H. Jiang, B. Wen, P. Kumar, J.L. Meagher, D. Sun, J.A. Stuckey, S. Wang, A. Potent, Selective Small-Molecule, Degrader of STAT3 achieves complete tumor regression, in: Vivo, Cancer Cell, vol. 36, 2019, pp. 498–511, e417.
[31] A.C. Lai, M. Toure, D. Hellerschmied, J. Salami, S. Jaime-Figueroa, E. Ko, J. Hines, C.M. Crews, Modular PROTAC design for the degradation of oncogenic BCR-ABL, in: Angew Chem Int (Ed.), Engl, vol. 55, 2016, pp. 807–810.
[32] W. McCoull, T. Cheung, E. Anderson, P. Barton, J. Burgess, K. Byth, Q. Cao, M.P. Castaldi, H. Chen, E. Chiarparin, R.J. Carbajo, E. Code, S. Cowan, P.R. Davey, A.D. Ferguson, S. Fillery, N.O. Fuller, N. Gao, D. Hargreaves, M.R. Howard, J. Hu, A. Kawatkar, P.D. Kemmitt, E. Leo, D.M. Molina, N. O'Connell, P. Petteruti, T. Rasmusson, P. Raubo, P.B. Rawlins, P. Ricchiuto, G.R. Robb, M. Schenone, M.J. Waring, M. Zinda, S. Fawell, D.M. Wilson, Development of a novel B-cell lymphoma 6 (BCL6) PROTAC to provide insight into small molecule targeting of BCL6, ACS Chem. Biol. 13 (2018) 3131–3141.
[33] M. Toure, C.M. Crews, Small-molecule PROTACS: new approaches to protein degradation, in: Angew Chem Int (Ed.), Engl, vol. 55, 2016, pp. 1966–1973.
[34] D.P. Bondeson, A. Mares, I.E. Smith, E. Ko, S. Campos, A.H. Miah, K.E. Mulholland, N. Routly, D.L. Buckley, J.L. Gustafson, N. Zinn, P. Grandi, S. Shimamura, G. Bergamini, M. Faelth-Savitski, M. Bantscheff, C. Cox, D.A. Gordon, R.R. Willard, J.J. Flanagan, L.N. Casillas, B.J. Votta, W. den Besten, K. Famm, L. Kruidenier, P.S. Carter, J.D. Harling, I. Churcher, C.M. Crews, Catalytic in vivo protein knockdown by small-molecule PROTACs, Nat. Chem. Biol. 11 (2015) 611–617.
[35] D.A. Ruess, G.J. Heynen, K.J. Ciecielski, J. Ai, A. Berninger, D. Kabacaoglu, K. Görgülü, Z. Dantes, S.M. Wörmann, K.N. Diakopoulos, A.F. Karpathaki, M. Kowalska, E. Kaya-Aksoy, L. Song, E.A.Z. van der Laan, M.P. Lopez-Alberca, M. Nazare , M. Reichert, D. Saur, M.M. Erkan, U.T. Hopt, B. Sainz, W. Birchmeier, R.M. Schmid, M. Lesina, H. Algül, Mutant KRASdriven cancers depend on PTPN11/SHP2 phosphatase, Nat. Med. 24 (2018) 954–960.
[36] M. Wang, J. Lu, M. Wang, C.Y. Yang, S. Wang, Discovery of SHP2-D26 as a first, potent, and effective PROTAC degrader of SHP2 protein, J. Med. Chem. 63 (2020) 7510–7528.
[37] M. Zengerle, K.H. Chan, A. Ciulli, Selective small molecule induced degradation of the BET bromodomain protein BRD4, ACS Chem. Biol. 10 (2015) 1770–1777.
[38] E.S. Fischer, K. Bohm, J.R. Lydeard, H. Yang, M.B. Stadler, S. Cavadini, J. Nagel, F. Serluca, V. Acker, G.M. Lingaraju, R.B. Tichkule, M. Schebesta, W.C. Forrester, M. Schirle, U. Hassiepen, J. Ottl, M. Hild, R.E. Beckwith, J.W. Harper, J.L. Jenkins, N.H. Thoma, Structure of the DDB1-CRBN E3 ubiquitin ligase in complex with thalidomide, Nature 512 (2014) 49–53.
[39] J. Adams, V.J. Palombella, E.A. Sausville, J. Johnson, A. Destree, D.D. Lazarus, J. Maas, C.S. Pien, S. Prakash, P.J. Elliott, Proteasome inhibitors: a novel class of potent and effective antitumor agents,, Canc. Res. 59 (1999) 2615–2622.